

Tetracarbon Metallo-carboranes. 2.¹ Thermal Rearrangement of 14-Vertex Cage Systems. Crystal Structures of Three Tetracarbon Diferracarborane Isomers, $(\eta^5\text{-C}_5\text{H}_5)_2\text{Fe}_2(\text{CH}_3)_4\text{C}_4\text{B}_8\text{H}_8$

William M. Maxwell, Richard Weiss, Ekk Sinn, and Russell N. Grimes*

Contribution from the Department of Chemistry, University of Virginia, Charlottesville, Virginia 22901. Received December 9, 1976

Abstract: The stereochemistry of 14-vertex polyhedral cages has been explored via a study of the crystal structures of several isomers of $(\eta^5\text{-C}_5\text{H}_5)_2\text{Fe}_2(\text{CH}_3)_4\text{C}_4\text{B}_8\text{H}_8$ and their thermal rearrangement. In contrast to other metallo-carborane systems, isomerism in these species involves changes in gross polyhedral geometry. Isomers I and II, formed by treatment of the $(\text{CH}_3)_4\text{C}_4\text{B}_8\text{H}_8^{2-}$ ion with FeCl_2 and NaC_5H_5 below 25 °C, have sharply different open-cage (nido) structures with a five- and a four-sided open face, respectively; these results violate the skeletal electron-count theory for polyhedral compounds, which predict closo geometry for this system. Both I and II rearrange below 170 °C to a common isomer, V, which has a structure similar to that of I with a BH and a CCH₃ unit interchanged. In I, II, and V the distribution of framework carbon atoms is unusual, with carbon residing in both low- and high-coordinate polyhedral vertices. Isomer V rearranges at 300 °C to still other isomers, VII and VIII, whose ¹¹B and ¹H NMR spectra (supported by an x-ray study in the case of VIII) indicate closo structures consisting of a bicapped hexagonal antiprism with the metal atoms in the capping locations. In VII, the arrangement of methyl groups produces C₂ symmetry, but VIII has pseudo-D_{2d} symmetry with all eight boron atoms equivalent. Continued heating of VII at 300 °C generates only VIII and decomposition products. In the conversion of V to VII two nonadjacent cage carbon atoms evidently migrate to adjacent vertices, indicating that the drive to achieve cage closure takes precedence over the normal tendency for framework carbons to separate from each other on thermal rearrangement. Crystal data: isomer I, space group P2₁/n, Z = 4, a = 10.676 (2), b = 14.009 (5), c = 13.667 (5) Å, β = 93.97 (3)°, V = 2039 Å³, and R = 4.1% for 2796 reflections; isomer II, space group C2/c, Z = 8, a = 16.338 (3), b = 8.210 (2), c = 31.55 (1) Å, β = 103.74 (2)°, V = 4111 Å³, and R = 4.2% for 2849 reflections; isomer V, space group P2₁/c, Z = 4, a = 14.805 (4), b = 10.547 (2), c = 14.682 (5) Å, β = 109.20 (2)°, V = 2060 Å³, and R = 4.7% for 1660 reflections.

The recent discovery of a series of tetracarbon carboranes including $(\text{CH}_3)_4\text{C}_4\text{B}_8\text{H}_8^{2,3a}$ and $(\text{CH}_3)_4\text{C}_4\text{B}_7\text{H}_7^{3b}$ and the subsequent development of a versatile tetracarbon metallo-carborane chemistry,^{1a} have provided us with opportunities to explore some new aspects of the stereochemistry of boron cages. One such area concerns the structure, bonding, and thermal rearrangement of polyhedra containing 14 vertices. Cages as large as this (which presently represent the outer limit for polyhedral molecules) are uncommon; the only example prior to this work is the $(\eta^5\text{-C}_5\text{H}_5)_2\text{Co}_2\text{C}_2\text{B}_{10}\text{H}_{12}$ system reported in 1974 by Evans and Hawthorne.⁴ In that work, closo geometries based on a bicapped hexagonal antiprism were postulated from NMR data for the two isomers reported, but the structures of these compounds have not yet received x-ray confirmation.

In the accompanying paper^{1a} we describe the synthesis of several 14-vertex diiron species, $(\eta^5\text{-C}_5\text{H}_5)_2\text{Fe}_2(\text{CH}_3)_4\text{C}_4\text{B}_8\text{H}_8$, from $(\text{CH}_3)_4\text{C}_4\text{B}_8\text{H}_8$ via reduction to the dianion and subsequent treatment with FeCl_2 and NaC_5H_5 . Four isomers of the diiron system were isolated as air-stable crystalline solids, designated respectively as I (brown), II (green-gray), III (gray-brown), and IV (gray),⁵ the last of these in only trace quantity. Subsequently we found that still other isomers are produced on rearrangement of the original compounds I and II at elevated temperature. Accordingly, detailed structural investigations of several of these compounds were carried out in conjunction with studies of their thermal interconversion. In this report we describe the results of the thermolysis experiments as well as x-ray structure determinations of three of the isomers, two of which have been discussed in a preliminary communication.⁷

Results and Discussion

Structures of Isomers I and II. The brown (I) and green (II) isomers of $(\eta^5\text{-C}_5\text{H}_5)_2\text{Fe}_2(\text{CH}_3)_4\text{C}_4\text{B}_8\text{H}_8$ were characterized initially from their ¹¹B and ¹H NMR, infrared, and mass

spectra.^{1a} Although the NMR data indicated low symmetry for both species, the isomers were expected to have the geometry of a bicapped hexagonal antiprism (Figure 1) with the metal atoms occupying the high-coordinate "capping" vertices; the observed absence of symmetry was ascribed to asymmetric placement of the CCH₃ units on the cages. Such a closo structure would be consistent with the well-established skeletal electron-counting rules⁸ for electron-deficient compounds, since the usual assignment of each BH group as a two-electron donor to the cage framework, each CCH₃ unit as a three-electron donor, and each $\text{Fe}(\text{C}_5\text{H}_5)$ moiety as a one-electron donor,⁸ would total 30 skeletal bonding electrons for a 14-vertex $\text{Fe}_2\text{C}_4\text{B}_8$ system. It has been shown from both qualitative⁸ and quantitative⁹ arguments that *n*-vertex polyhedra containing $2n + 2$ framework bonding electrons will normally adopt closo structures in which all faces on the polyhedron are triangular. The geometry in Figure 1 is not the only possibility for a 14-vertex closo system (another is the hexacapped cube suggested by Lipscomb¹⁰ for a hypothetical $\text{B}_{14}\text{H}_{14}^{2-}$ ion), but it appeared a priori most reasonable for a metallo-carborane in light of the established structures of smaller polyhedra.¹¹ As previously noted, this geometry was proposed earlier for the dicobalt species $(\text{C}_5\text{H}_5)_2\text{Co}_2\text{C}_2\text{B}_{10}\text{H}_{12}$, which in fact are iso-electronic analogues of I and II.

The actual molecular structures of I and II are depicted in Figures 2 and 3, with packing diagrams in Figures 4 and 5. Positional and thermal parameters are listed in Tables I and II, bond distances in Table IV, and bond angles in Table V. The structures shown clearly do not reflect the expected geometry as described above, and are in fact nido (open-sided) cages. In I, the ring of atoms formed by B9, C12, B13, C14, and C11 is an open face, as shown by the long transannular distances; the shortest of these is 2.577 (4) Å between B9 and B13, and the longest is 2.880 (3) Å for C11-C12, all being clearly non-bonding interactions. In isomer II, the nonbonding distances of 2.564 (5) Å for B9-C14 and 2.765 (3) Å for Fe7-C11 define

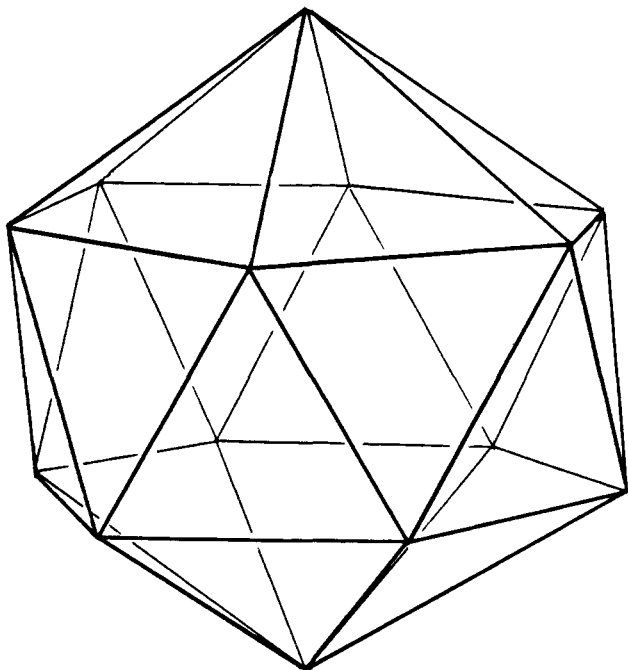


Figure 1. Bicapped hexagonal antiprism.

B9-Fe7-C14-C11 as an open face. The polyhedron in II also contains some distances which are unusually long, but still regarded as bonding; these are B10-B1 [1.998 (6)], B(13)-B(1) [2.095 (6)], Fe7-B9 [2.247 (4)], and Fe7-B10 [2.307 (4) Å].

Another unusual feature in I and II is the arrangement of cage carbon atoms. While the precursor molecule $(\text{CH}_3)_4\text{C}_4\text{B}_8\text{H}_8$ has all four carbons in a contiguous chain,^{1a,3a} and the $(\text{CH}_3)_4\text{C}_4\text{B}_8\text{H}_8^{2-}$ dianion^{1a} almost certainly retains at least two of the polyhedral C-C links intact (perhaps breaking the central C-C bond to form two separate C-C units on the polyhedral surface), in complexes I and II only one C-C link remains. Moreover, in I there are three carbons on the open face, while the fourth carbon (C4) is as far removed as possible from the open face; in II, only two carbons are located on the open side. A further observation, which is contrary to the normal expectation¹² that cage carbon atoms prefer low-coordinate locations, is that in both isomers, three of the C-CH₃ units occupy four-coordinate vertices and the fourth is in a five-coordinate position. Finally, there are some remarkable differences between the two structures. If the CCH₃ groups are ignored (or if B13 and C4-CM4 are interchanged), I has a mirror plane perpendicular to the open face and passing through B9, B3, C4, and B10; only two six-coordinate vertices are present, both occupied by iron. Isomer II, in contrast, is a highly irregular polyhedron (which would have no symmetry even if identical units were placed at all 14 vertices) and contains three six-coordinate atoms of which two are iron and the other (B1) is boron.

Thus, the structures of I and II differ drastically not only from the expected closo polyhedron in Figure 1, but also from each other. Since the syntheses were conducted below 25 °C, it appeared that the geometry of these cages must be dictated largely by kinetic factors, especially the details of metal insertion into the carborane dianion. What was not obvious, however, was the reason for the failure to achieve the predicted closo structure. Two explanations seemed conceivable: either

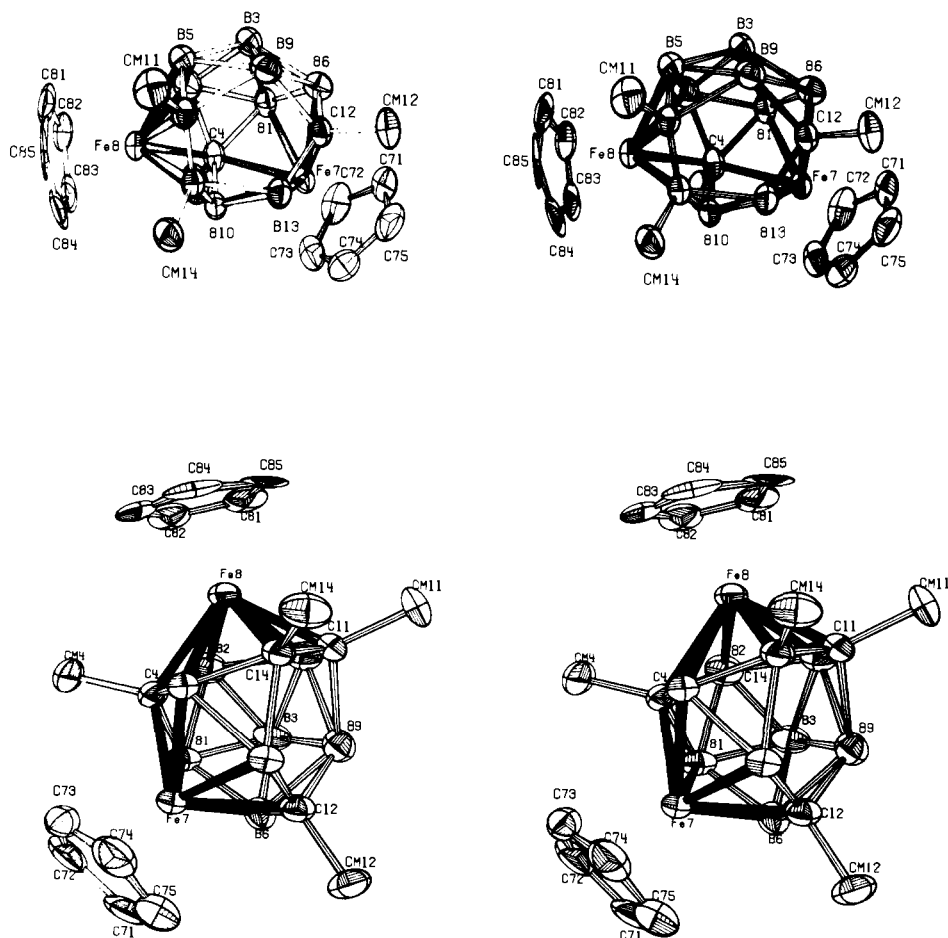


Figure 2. Two stereoviews of the molecular structure of $(\eta^5\text{-C}_5\text{H}_5)_2\text{Fe}_2(\text{CH}_3)_4\text{C}_4\text{B}_8\text{H}_8$, isomer I. The upper view is nearly normal to the five-sided open face.

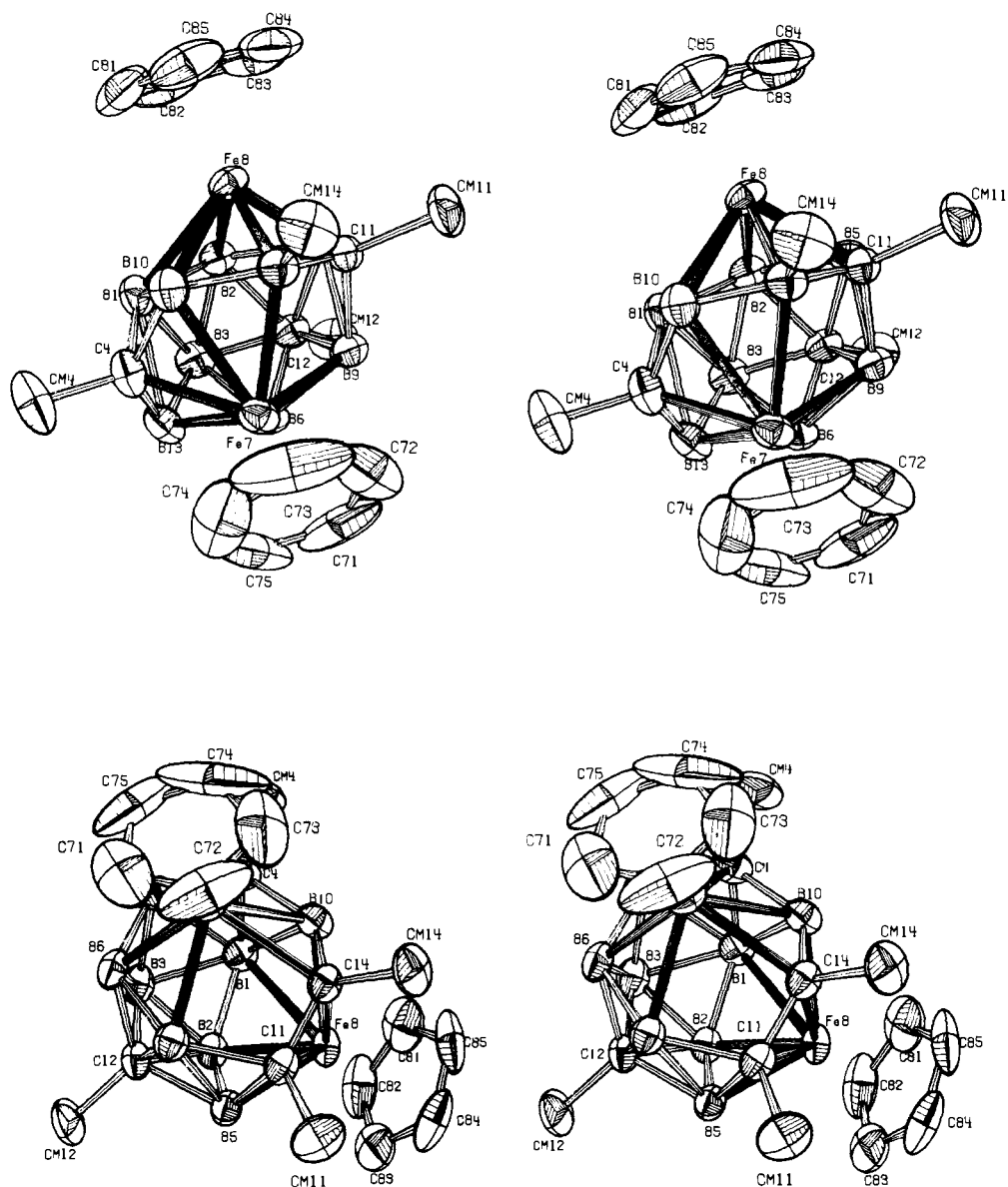


Figure 3. Two stereoviews of the molecular structure of $(\eta^5\text{-C}_5\text{H}_5)_2\text{Fe}_2(\text{CH}_3)_4\text{C}_4\text{B}_8\text{H}_8$, isomer II. The lower view is approximately normal to the four-sided open face.

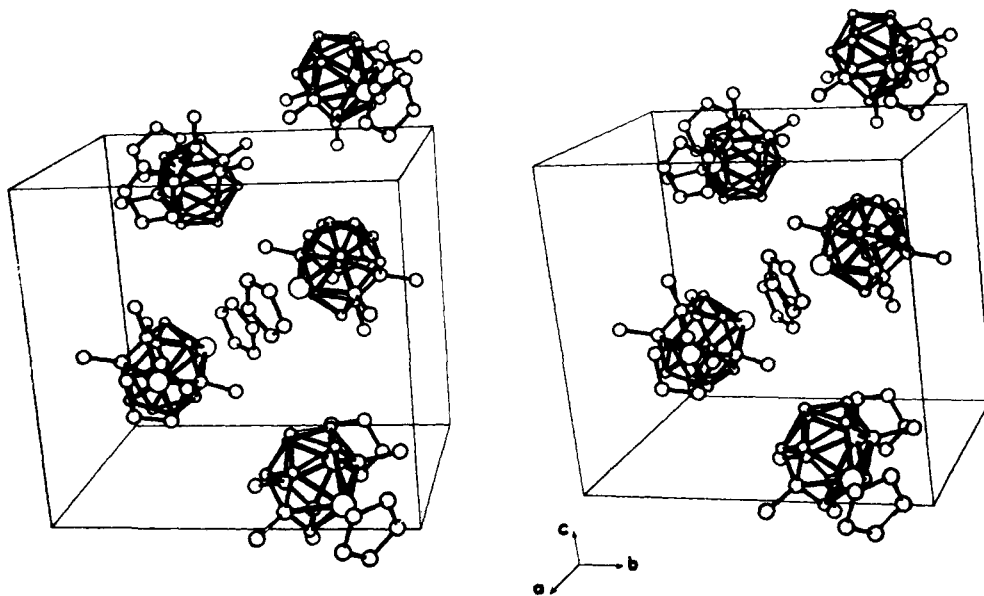


Figure 4. Packing diagram of isomer I.

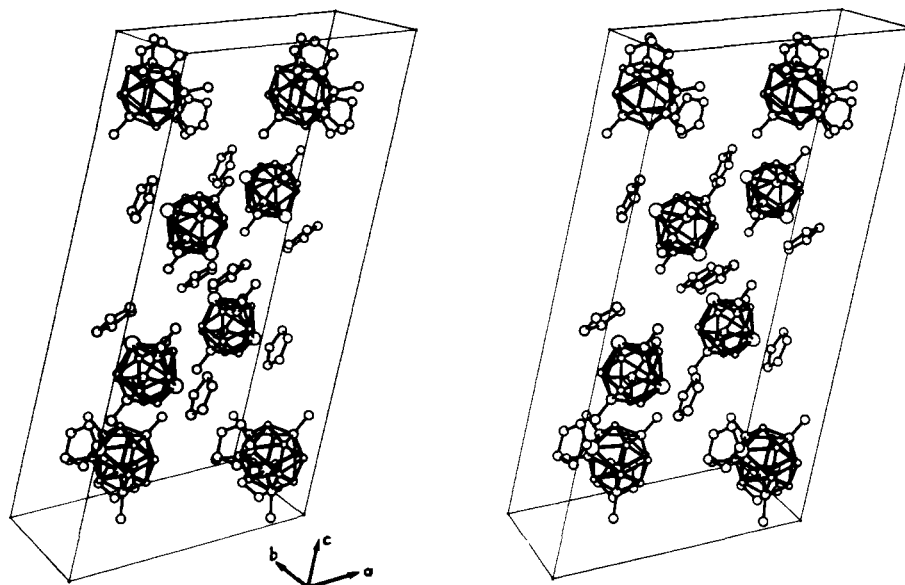


Figure 5. Packing diagram of isomer II.

the nido structures of I and II are prevented by high activation energy of rearrangement from reaching the closo configuration under reaction conditions, or else the closo geometry of Figure 1 is not, after all, thermodynamically favored and the skeletal electron-count theory fails for 14-vertex systems. In order to explore this question the behavior of I and II was examined at elevated temperature.

Rearrangement of Isomers I and II. Thermal isomerization studies of both isomers were conducted in *n*-nonane solution in sealed tubes, with periodic monitoring by ^{11}B NMR to check for the appearance of new isomers; however, no attempts were made to determine the lowest possible temperatures at which rearrangements could occur. It was found that I converts quantitatively at 170°C to a new isomer, V, with no evidence of any isolable intermediate. Isomer II, on heating at 140°C , rearranges initially to still another species, VI; on continued thermolysis at that temperature, VI rearranges further to give V, the same product obtained from I. Thus, while the original isomers I and II do not interconvert, they do rearrange to a common species, V. The intermediate VI was observed only via proton NMR, but V was isolated as a gray solid and characterized from its ^{11}B , ^1H , and mass spectra (see Experimental Section).

Structure of Isomer V. An x-ray crystallographic study of V revealed the geometry shown in Figures 6 and 7, with positional and thermal parameters listed in Table III and selected distances and angles in Tables IV(c) and V(c). The structure is closely related to that of I (Figure 2), and in fact I and V basically differ only in the location of one CCH_3 unit. Both isomers contain a five-sided open face, that in V being defined by B9, C12, B13, C14, and B11; the distance B11–B13 in V is 2.241 (4) Å, which might be considered weakly bonding, but for purposes of this discussion we shall regard it as nonbonding in order to facilitate comparison with I. The remaining transannular distances in the open face range from 2.544 (5) Å for B9–B13 to 3.014 (5) Å for B9–C14, and are clearly nonbonding. With the aid of a common numbering system for I and V, it can be seen that the interchange of BH and CCH_3 units at positions 3 and 11 converts I into V (this denotes a formal relationship and does not imply an actual mechanism). It is significant that the conversion of I to V effectively removes the only direct C–C contact on the polyhedral surface and is consistent with the usual tendency of cage carbon atoms to prefer nonadjacent locations.^{11,12} However, we have noted earlier that the tendency of carbon atoms in carboranes to occupy low-coordinate vertices is not obvious in I and II; even

more remarkable is the fact that in the rearrangement product V, the number of low-coordinate carbons has actually decreased to two. Thus, it appears that *the coordination number of framework carbon atoms is less important than the achievement of mutual separation* in determining the structures of these large systems. This is not, however, the end of the story, since the separation of carbon atoms is itself secondary to the achievement of a closo structure, as shown in the following observations.

Rearrangement of Isomer V. Since V was formed by isomerization of both I and II—species which are sharply dissimilar—it appeared possible that V, despite its nido geometry, might in fact be the thermodynamically most stable isomer. As a test of this conjecture, V was heated in *n*-nonane at progressively higher temperatures. After several hours at 200 and 220°C no change was observed as monitored by ^{11}B NMR spectroscopy, but thermolysis at 300°C for 1 h produced almost complete conversion to two new isomers, violet VII and green VIII, with VII predominant. The ^{11}B and ^1H spectra of VII and VIII indicated structures possessing symmetry, in contrast to the isomers described above. Thus, VII was seen to have equivalent $(\text{C}_5\text{H}_5)\text{Fe}$ groups, pairs of equivalent CCH_3 units, and four kinds of boron in a 2:2:2:2 pattern; in VIII, the spectra revealed the equivalence of both $(\text{C}_5\text{H}_5)\text{Fe}$ moieties, all CCH_3 groups, and all eight boron atoms. Only one structure seemed plausible for VIII: the bicapped hexagonal antiprism (Figure 1) with metal atoms in the capping locations and the CCH_3 groups in alternating positions on the equatorial rings as shown in Figure 8. This geometry has been confirmed in an x-ray crystal structure determination which will be reported elsewhere.¹³

For isomer VII, the pattern of equivalence indicated by the NMR data also points to a bicapped hexagonal antiprism with both iron atoms in the capping locations, but with a different arrangement of C– CH_3 units as compared to VIII. Six possible isomers (excluding enantiomers) are compatible with the spectra, but four of these have two or more direct C–C interactions and are regarded as unlikely in view of the fact that the precursor species V has *no* C–C bonds on the cage and the formation of two C–C links during thermal rearrangement would not be expected. The two remaining possibilities have their four C atoms in, respectively, the 2,4,9,11 and 2,4,10,12 locations, each with C_2 symmetry; of these, the 2,4,10,12 (shown in Figure 8) seems slightly more consistent with the very narrow range of ^{11}B chemical shifts (7 ppm). (The 2,4,9,11 isomer, with two boron atoms adjacent to three car-

Table I. Positional and Thermal Parameters and Estimated Standard Deviations for $Cp_2Fe_2Me_4C_4B_8H_8$ (isomer I)^a

| Atom | x | y | z | β_{11} | β_{22} | β_{33} | β_{12} | β_{13} | β_{23} |
|------|--------------|-------------|--------------|--------------|--------------|--------------|--------------|--------------|--------------|
| Fe7 | 0.16081 (5) | 0.17437 (4) | -0.13231 (4) | 0.00339 (5) | 0.00324 (3) | 0.00363 (3) | 0.00051 (7) | 0.00160 (7) | -0.00006 (5) |
| Fe8 | -0.18688 (5) | 0.23905 (4) | -0.14560 (4) | 0.00296 (5) | 0.00375 (3) | 0.00337 (3) | -0.00026 (7) | 0.00036 (7) | -0.00058 (6) |
| C4 | -0.0282 (4) | 0.1537 (3) | -0.1909 (3) | 0.0041 (4) | 0.0035 (2) | 0.0042 (2) | -0.0006 (5) | 0.0007 (5) | -0.0026 (4) |
| C11 | -0.0932 (4) | 0.3650 (3) | -0.1118 (3) | 0.0039 (4) | 0.0031 (2) | 0.0034 (2) | 0.0001 (5) | 0.0010 (5) | -0.0006 (4) |
| C12 | 0.1705 (4) | 0.3233 (3) | -0.1158 (3) | 0.0044 (4) | 0.0034 (2) | 0.0033 (2) | -0.0002 (5) | 0.0010 (5) | -0.0007 (4) |
| C14 | -0.0655 (4) | 0.2905 (3) | -0.0390 (3) | 0.0031 (3) | 0.0035 (2) | 0.0029 (2) | -0.0003 (5) | 0.0011 (5) | -0.0008 (4) |
| CM4 | -0.0630 (5) | 0.0470 (3) | -0.2113 (4) | 0.0068 (5) | 0.0037 (2) | 0.0085 (4) | -0.0027 (6) | 0.0011 (7) | -0.0047 (5) |
| CM11 | -0.1512 (5) | 0.4586 (3) | -0.0787 (4) | 0.0077 (5) | 0.0031 (2) | 0.0062 (3) | 0.0034 (6) | 0.0017 (7) | -0.0020 (5) |
| CM12 | 0.2923 (4) | 0.3786 (4) | -0.0818 (4) | 0.0040 (4) | 0.0053 (3) | 0.0058 (3) | -0.0027 (6) | 0.0008 (6) | -0.0022 (5) |
| CM14 | -0.1033 (4) | 0.3051 (4) | 0.0671 (3) | 0.0062 (4) | 0.0069 (3) | 0.0028 (2) | 0.0001 (7) | 0.0032 (5) | -0.0009 (5) |
| C71 | 0.3373 (5) | 0.1228 (4) | -0.1635 (4) | 0.0056 (4) | 0.0071 (3) | 0.0073 (3) | 0.0052 (7) | 0.0050 (7) | 0.0017 (6) |
| C72 | 0.2470 (5) | 0.0486 (4) | -0.1735 (4) | 0.0081 (5) | 0.0054 (3) | 0.0092 (4) | 0.0073 (7) | -0.0007 (8) | -0.0047 (6) |
| C73 | 0.1994 (5) | 0.0370 (3) | -0.0803 (5) | 0.0064 (5) | 0.0038 (3) | 0.0111 (4) | 0.0022 (6) | 0.0045 (8) | 0.0050 (6) |
| C74 | 0.2575 (5) | 0.1013 (4) | -0.0150 (4) | 0.0085 (5) | 0.0057 (3) | 0.0064 (3) | 0.0049 (7) | 0.0005 (7) | 0.0035 (5) |
| C75 | 0.3423 (5) | 0.1545 (4) | -0.0661 (4) | 0.0053 (5) | 0.0060 (3) | 0.0094 (4) | 0.0025 (7) | -0.0040 (7) | 0.0023 (6) |
| C81 | -0.3676 (5) | 0.2704 (4) | -0.1996 (5) | 0.0033 (4) | 0.0067 (3) | 0.0101 (4) | 0.0003 (7) | -0.0024 (7) | 0.0044 (6) |
| C82 | -0.3441 (5) | 0.1756 (4) | -0.2181 (4) | 0.0042 (4) | 0.0071 (3) | 0.0062 (3) | -0.0026 (7) | -0.0010 (6) | -0.0024 (6) |
| C83 | -0.3199 (4) | 0.1285 (4) | -0.1299 (4) | 0.0039 (4) | 0.0051 (3) | 0.0091 (4) | -0.0022 (6) | 0.0014 (7) | 0.0013 (6) |
| C84 | -0.3275 (5) | 0.1928 (5) | -0.0546 (4) | 0.0037 (4) | 0.0114 (5) | 0.0058 (3) | -0.0047 (8) | 0.0039 (6) | 0.0013 (7) |
| C85 | -0.3577 (5) | 0.2824 (4) | -0.0958 (5) | 0.0032 (4) | 0.0074 (3) | 0.0112 (4) | -0.0014 (7) | 0.0047 (7) | -0.0071 (7) |
| B1 | 0.0700 (5) | 0.1988 (4) | -0.2711 (3) | 0.0055 (5) | 0.0051 (3) | 0.0028 (2) | 0.0001 (7) | 0.0015 (6) | -0.0024 (5) |
| B2 | -0.0910 (5) | 0.2313 (4) | -0.2752 (4) | 0.0052 (5) | 0.0058 (3) | 0.0027 (3) | 0.0001 (7) | 0.0002 (6) | -0.0018 (5) |
| B3 | 0.0239 (5) | 0.3173 (4) | -0.2951 (3) | 0.0059 (5) | 0.0063 (3) | 0.0025 (2) | 0.0011 (7) | 0.0018 (6) | 0.0014 (5) |
| B5 | -0.1042 (5) | 0.3490 (4) | -0.2292 (4) | 0.0048 (4) | 0.0043 (3) | 0.0034 (3) | 0.0012 (6) | 0.0007 (6) | 0.0015 (5) |
| B6 | 0.1688 (5) | 0.2930 (4) | -0.2284 (3) | 0.0052 (5) | 0.0038 (3) | 0.0032 (3) | 0.0000 (6) | 0.0027 (6) | 0.0001 (5) |
| B9 | 0.0567 (5) | 0.3845 (4) | -0.1843 (4) | 0.0054 (5) | 0.0035 (3) | 0.0040 (3) | 0.0001 (6) | 0.0026 (6) | 0.0008 (5) |
| B10 | -0.0182 (5) | 0.1834 (3) | -0.0720 (3) | 0.0034 (4) | 0.0035 (3) | 0.0035 (3) | -0.0005 (6) | 0.0013 (6) | 0.0010 (4) |
| B13 | 0.1004 (5) | 0.2741 (4) | -0.0350 (4) | 0.0032 (4) | 0.0040 (3) | 0.0036 (3) | 0.0004 (6) | 0.0006 (6) | 0.0003 (5) |
| H71 | 0.390 (5) | 0.150 (3) | -0.216 (3) | 5.0 | | | | | |
| H72 | 0.220 (5) | 0.013 (4) | -0.237 (3) | 5.0 | | | | | |
| H73 | 0.135 (5) | -0.011 (3) | -0.064 (3) | 5.0 | | | | | |
| H74 | 0.241 (5) | 0.113 (4) | 0.057 (3) | 5.0 | | | | | |
| H75 | 0.399 (5) | 0.209 (4) | -0.036 (4) | 5.0 | | | | | |
| H81 | -0.389 (5) | 0.321 (3) | -0.250 (3) | 5.0 | | | | | |
| H82 | -0.344 (5) | 0.145 (3) | -0.286 (3) | 5.0 | | | | | |
| H83 | -0.303 (5) | 0.060 (3) | -0.122 (3) | 5.0 | | | | | |
| H84 | -0.311 (5) | 0.179 (3) | 0.018 (3) | 5.0 | | | | | |
| H85 | -0.368 (5) | 0.343 (3) | -0.060 (3) | 5.0 | | | | | |
| H1B | 0.082 (5) | 0.163 (3) | -0.328 (4) | 5.2 (9) | | | | | |
| H2B | -0.144 (5) | 0.216 (3) | -0.337 (3) | 4.6 (9) | | | | | |
| H3B | 0.016 (4) | 0.342 (3) | -0.364 (3) | 4.5 (9) | | | | | |
| H5B | -0.163 (4) | 0.402 (3) | -0.265 (3) | 2.8 (9) | | | | | |
| H6B | 0.256 (4) | 0.310 (3) | -0.258 (3) | 2.9 (9) | | | | | |
| H9B | 0.093 (6) | 0.475 (4) | -0.181 (4) | 7.4 (9) | | | | | |
| H10B | -0.039 (4) | 0.128 (3) | -0.017 (3) | 2.2 (9) | | | | | |
| H13B | 0.138 (5) | 0.259 (3) | 0.054 (3) | 4.6 (9) | | | | | |

^a The form of the anisotropic thermal parameter is: $\exp[-(\beta_{11}h^2 + \beta_{22}k^2 + \beta_{33}l^2 + \beta_{12}hk + \beta_{13}hl + \beta_{23}kl)]$.

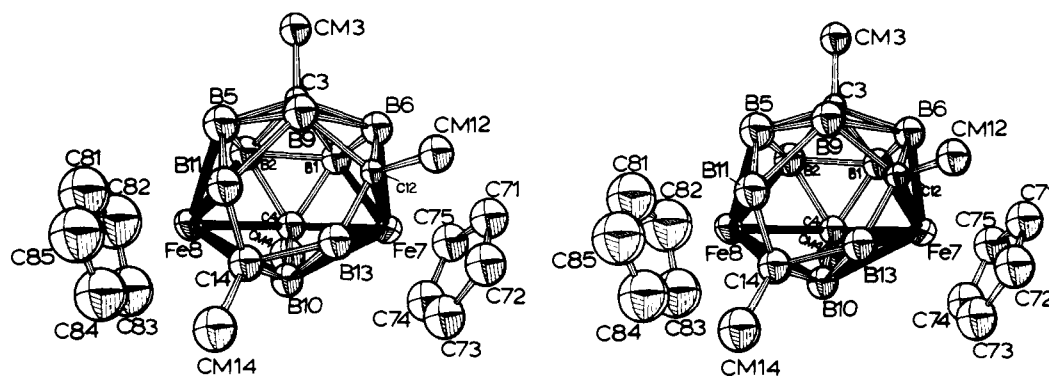


Figure 6. Stereoview of the molecular structure of $(\eta^5-C_5H_5)_2Fe_2(CH_3)_4C_4B_8H_8$, isomer V; view is approximately normal to the five-sided open face.

bons, would have a less uniform set of boron environments than the 2,4,10,12 and hence should presumably exhibit a larger range of chemical shifts, but this is admittedly a marginal judgment.)

It will be noted that both the 2,4,9,11 and 2,4,10,12 isomers each have one carbon-carbon bond in the cage framework. Interestingly, there are no possible structures for VII consistent with the NMR data and having all cage carbons nonadjacent,

Table II. Positional and Thermal Parameters and Estimated Standard Deviations for $Cp_2Fe_2Me_4C_4B_8H_8$ (isomer II)^a

| Atom | x | y | z | β_{11} | β_{22} | β_{33} | β_{12} | β_{13} | β_{23} |
|------|-------------|-------------|-------------|--------------|--------------|---------------|--------------|--------------|--------------|
| Fe7 | 0.12847 (5) | 0.26220 (9) | 0.07941 (2) | 0.00291 (3) | 0.0089 (1) | 0.000 595 (7) | -0.0012 (1) | 0.00001 (2) | 0.00060 (5) |
| Fe8 | 0.30087 (4) | 0.09692 (9) | 0.16484 (2) | 0.00173 (2) | 0.0076 (1) | 0.000 837 (7) | -0.0001 (1) | 0.00056 (2) | 0.00083 (5) |
| C4 | 0.1728 (3) | 0.0305 (7) | 0.0694 (2) | 0.0043 (2) | 0.0096 (8) | 0.000 70 (5) | -0.0022 (8) | 0.0012 (2) | -0.0013 (4) |
| C11 | 0.2329 (3) | 0.3142 (6) | 0.1611 (2) | 0.0023 (2) | 0.0056 (7) | 0.000 70 (5) | -0.0010 (6) | 0.0003 (2) | -0.0001 (3) |
| C12 | 0.1081 (3) | 0.0953 (6) | 0.1713 (2) | 0.0021 (2) | 0.0098 (8) | 0.000 78 (5) | -0.0010 (7) | 0.0000 (2) | 0.0005 (4) |
| C14 | 0.2585 (3) | 0.2855 (6) | 0.1209 (2) | 0.0024 (2) | 0.0071 (7) | 0.000 74 (5) | -0.0019 (7) | 0.0004 (2) | 0.0006 (3) |
| C4M | 0.1823 (5) | -0.0565 (9) | 0.0273 (2) | 0.0075 (4) | 0.0200 (12) | 0.000 93 (6) | -0.0053 (12) | 0.0022 (2) | -0.0041 (5) |
| C11M | 0.2626 (4) | 0.4758 (7) | 0.1863 (2) | 0.0047 (3) | 0.0076 (8) | 0.001 05 (6) | -0.0032 (8) | 0.0005 (2) | -0.0020 (4) |
| C12M | 0.0545 (3) | 0.0849 (8) | 0.2053 (2) | 0.0030 (2) | 0.0221 (12) | 0.001 0 (6) | -0.0018 (9) | 0.0019 (2) | 0.0017 (5) |
| C14M | 0.3199 (3) | 0.4122 (7) | 0.1088 (2) | 0.0039 (2) | 0.0126 (9) | 0.001 19 (6) | -0.0065 (8) | 0.0015 (2) | 0.0017 (4) |
| C71 | 0.0314 (5) | 0.4210 (10) | 0.0594 (2) | 0.0065 (3) | 0.0369 (16) | 0.001 86 (9) | 0.0196 (12) | 0.0026 (3) | 0.0113 (6) |
| C72 | 0.1043 (6) | 0.5047 (8) | 0.0659 (2) | 0.0120 (6) | 0.0102 (10) | 0.001 45 (9) | -0.0047 (14) | -0.0037 (4) | 0.0038 (5) |
| C73 | 0.1453 (5) | 0.4451 (11) | 0.0372 (2) | 0.0051 (3) | 0.0579 (18) | 0.002 56 (9) | 0.0043 (15) | 0.0020 (3) | 0.0212 (5) |
| C74 | 0.0996 (8) | 0.3309 (12) | 0.0139 (2) | 0.0225 (8) | 0.0378 (19) | 0.000 58 (7) | 0.0357 (19) | 0.0024 (4) | 0.0032 (6) |
| C75 | 0.0309 (5) | 0.3135 (9) | 0.0275 (2) | 0.0092 (4) | 0.0191 (13) | 0.001 86 (10) | -0.0098 (14) | -0.0057 (3) | 0.0050 (6) |
| C81 | 0.4007 (4) | -0.0560 (9) | 0.1617 (2) | 0.0033 (2) | 0.0194 (12) | 0.002 07 (10) | 0.0062 (10) | 0.0014 (3) | -0.0007 (6) |
| C82 | 0.3739 (4) | -0.0861 (8) | 0.1997 (2) | 0.0026 (2) | 0.0163 (11) | 0.002 40 (11) | 0.0035 (9) | 0.0005 (3) | 0.0064 (6) |
| C83 | 0.3845 (4) | 0.0546 (10) | 0.2246 (2) | 0.0025 (2) | 0.0309 (15) | 0.001 0 (7) | 0.0040 (11) | -0.0003 (2) | 0.0028 (6) |
| C84 | 0.4179 (4) | 0.1735 (8) | 0.2014 (2) | 0.0020 (2) | 0.0166 (11) | 0.002 11 (11) | -0.0013 (9) | -0.0012 (3) | 0.0005 (6) |
| C85 | 0.4282 (3) | 0.1043 (9) | 0.1629 (2) | 0.0021 (2) | 0.0235 (13) | 0.002 08 (9) | 0.0006 (10) | 0.0020 (2) | 0.0040 (6) |
| B1 | 0.2033 (4) | -0.0696 (7) | 0.1194 (2) | 0.0033 (2) | 0.0077 (9) | 0.000 85 (6) | -0.0016 (8) | 0.0010 (2) | -0.0011 (4) |
| B2 | 0.1953 (4) | -0.0289 (7) | 0.1738 (2) | 0.0025 (2) | 0.0080 (8) | 0.000 7 (6) | -0.0004 (8) | 0.0006 (2) | 0.0013 (4) |
| B3 | 0.0994 (4) | -0.0574 (8) | 0.1362 (2) | 0.0026 (2) | 0.0094 (9) | 0.001 03 (7) | -0.0029 (8) | 0.0009 (2) | 0.0007 (4) |
| B5 | 0.2044 (3) | 0.1748 (7) | 0.1921 (2) | 0.0021 (2) | 0.0097 (9) | 0.000 53 (5) | -0.0010 (8) | 0.0003 (2) | 0.0003 (4) |
| B6 | 0.0584 (4) | 0.1390 (8) | 0.1187 (2) | 0.0018 (2) | 0.0118 (10) | 0.000 87 (6) | -0.0016 (8) | 0.0002 (2) | 0.0003 (4) |
| B9 | 0.1245 (3) | 0.2868 (7) | 0.1498 (2) | 0.0023 (2) | 0.0084 (9) | 0.000 73 (6) | 0.0007 (8) | 0.0004 (2) | 0.0002 (4) |
| B10 | 0.2534 (4) | 0.1184 (8) | 0.0942 (2) | 0.0031 (2) | 0.0106 (10) | 0.000 71 (6) | -0.0007 (9) | 0.0013 (2) | -0.0002 (4) |
| B13 | 0.0873 (4) | 0.0093 (8) | 0.0810 (2) | 0.0039 (3) | 0.0114 (10) | 0.000 68 (6) | -0.0032 (10) | 0.0000 (2) | -0.0006 (4) |
| H71 | -0.008 (3) | 0.445 (7) | 0.075 (2) | 5 | | | | | |
| H72 | 0.121 (3) | 0.584 (7) | 0.087 (2) | 5 | | | | | |
| H73 | 0.195 (4) | 0.486 (7) | 0.034 (2) | 5 | | | | | |
| H74 | 0.105 (3) | 0.263 (7) | -0.009 (2) | 5 | | | | | |
| H75 | -0.011 (4) | 0.243 (7) | 0.017 (2) | 5 | | | | | |
| H81 | 0.400 (3) | -0.130 (7) | 0.139 (2) | 5 | | | | | |
| H82 | 0.356 (3) | -0.181 (7) | 0.206 (2) | 5 | | | | | |
| H83 | 0.374 (4) | 0.065 (7) | 0.249 (2) | 5 | | | | | |
| H84 | 0.427 (3) | 0.271 (7) | 0.211 (2) | 5 | | | | | |
| H85 | 0.444 (4) | 0.162 (7) | 0.140 (2) | 5 | | | | | |
| H1B | 0.230 (3) | -0.188 (6) | 0.115 (1) | 3 (1) | | | | | |
| H2B | 0.204 (3) | -0.104 (6) | 0.199 (2) | 4 (1) | | | | | |
| H3B | 0.058 (3) | -0.160 (6) | 0.142 (2) | 3 (1) | | | | | |
| H5B | 0.212 (3) | 0.207 (5) | 0.227 (1) | 2 (1) | | | | | |
| H6B | -0.005 (3) | 0.163 (7) | 0.116 (2) | 5 (1) | | | | | |
| H9B | 0.095 (3) | 0.385 (5) | 0.163 (1) | 2 (1) | | | | | |
| H10B | 0.304 (3) | 0.106 (6) | 0.078 (2) | 3 (1) | | | | | |
| H13B | 0.035 (3) | -0.057 (6) | 0.056 (2) | 4 (1) | | | | | |

^a The form of the anisotropic thermal parameter is: $\exp[-(\beta_{11}h^2 + \beta_{22}k^2 + \beta_{33}l^2 + \beta_{12}hk + \beta_{13}hl + \beta_{23}kl)]$.

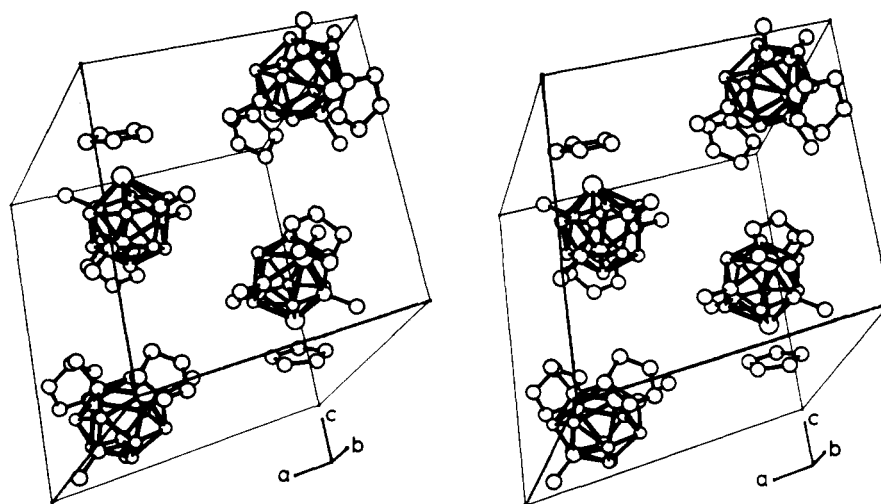


Figure 7. Packing diagram of isomer V.

Table III. Positional and Thermal Parameters and Estimated Standard Deviations for $Cp_2Fe_2Me_4C_4B_8H_8$ (isomer V)^a

| Atom | x | y | z | β_{11} | β_{22} | β_{33} | β_{12} | β_{13} | β_{23} |
|------|-------------|-------------|-------------|--------------|--------------|--------------|--------------|--------------|--------------|
| Fe7 | 0.20870 (9) | 0.4103 (1) | 0.24641 (8) | 0.00414 (6) | 0.0061 (1) | 0.00296 (5) | -0.0016 (2) | 0.00266 (9) | -0.0017 (2) |
| Fe8 | 0.28197 (9) | 0.7398 (1) | 0.32136 (8) | 0.00485 (7) | 0.0039 (1) | 0.00456 (6) | 0.0006 (2) | 0.00411 (10) | 0.0007 (2) |
| C71 | 0.1431 (7) | 0.2377 (9) | 0.1633 (6) | 0.0084 (7) | 0.0089 (10) | 0.0053 (5) | -0.008 (2) | 0.0044 (10) | -0.007 (1) |
| C72 | 0.2421 (8) | 0.2404 (10) | 0.1604 (7) | 0.0097 (8) | 0.0095 (11) | 0.0064 (6) | -0.001 (2) | 0.0050 (10) | -0.008 (1) |
| C73 | 0.2519 (7) | 0.3385 (10) | 0.1013 (7) | 0.0083 (7) | 0.0139 (13) | 0.0062 (6) | -0.006 (2) | 0.0081 (9) | -0.009 (1) |
| C74 | 0.1582 (8) | 0.3977 (10) | 0.0671 (6) | 0.0106 (8) | 0.0108 (11) | 0.0026 (5) | -0.003 (2) | 0.0020 (10) | -0.004 (1) |
| C75 | 0.0912 (7) | 0.3374 (9) | 0.1054 (6) | 0.0056 (6) | 0.0117 (11) | 0.0034 (5) | -0.003 (2) | 0.0013 (9) | -0.003 (1) |
| C81 | 0.2811 (10) | 0.9057 (10) | 0.3909 (7) | 0.0286 (12) | 0.0046 (10) | 0.0116 (6) | -0.000 (2) | 0.0281 (12) | -0.004 (2) |
| C82 | 0.2127 (8) | 0.9146 (10) | 0.3049 (11) | 0.0050 (7) | 0.0053 (11) | 0.0284 (17) | 0.004 (2) | 0.0049 (18) | 0.004 (2) |
| C83 | 0.2627 (15) | 0.9043 (10) | 0.2393 (8) | 0.0404 (25) | 0.0054 (11) | 0.0042 (7) | -0.008 (3) | 0.0010 (22) | 0.004 (2) |
| C84 | 0.3583 (9) | 0.8913 (10) | 0.2941 (9) | 0.0218 (8) | 0.0037 (10) | 0.0280 (10) | -0.006 (2) | 0.0414 (11) | 0.000 (2) |
| C85 | 0.3662 (10) | 0.8896 (10) | 0.3830 (10) | 0.0133 (12) | 0.0050 (11) | 0.0154 (11) | -0.001 (2) | -0.0108 (20) | -0.001 (2) |
| C3 | 0.1678 (5) | 0.5213 (8) | 0.3989 (5) | 0.0044 (4) | 0.0063 (9) | 0.0034 (4) | 0.001 (1) | 0.0060 (6) | 0.000 (1) |
| C4 | 0.1738 (6) | 0.6076 (7) | 0.2266 (5) | 0.0039 (5) | 0.0044 (8) | 0.0029 (4) | 0.001 (1) | 0.0022 (7) | 0.002 (1) |
| C12 | 0.3029 (6) | 0.3697 (7) | 0.3565 (6) | 0.0039 (5) | 0.0050 (8) | 0.0034 (4) | 0.001 (1) | 0.0020 (7) | 0.001 (1) |
| C14 | 0.3834 (5) | 0.6074 (7) | 0.3139 (5) | 0.0028 (4) | 0.0034 (8) | 0.0052 (5) | -0.000 (1) | 0.0028 (7) | -0.002 (1) |
| C3M | 0.0950 (6) | 0.5099 (10) | 0.4616 (6) | 0.0088 (5) | 0.0149 (14) | 0.0071 (5) | -0.000 (2) | 0.0146 (7) | 0.001 (1) |
| C4M | 0.0964 (7) | 0.6707 (9) | 0.1354 (6) | 0.0057 (6) | 0.0096 (11) | 0.0047 (6) | 0.003 (2) | 0.0002 (10) | 0.005 (1) |
| C12M | 0.3492 (7) | 0.2357 (8) | 0.3905 (6) | 0.0072 (6) | 0.0031 (8) | 0.0071 (6) | 0.004 (1) | 0.0044 (10) | 0.004 (1) |
| C14M | 0.4860 (6) | 0.6442 (9) | 0.2992 (7) | 0.0049 (5) | 0.0082 (10) | 0.0092 (6) | -0.003 (1) | 0.0078 (9) | 0.001 (1) |
| B1 | 0.1150 (7) | 0.5035 (10) | 0.2765 (7) | 0.0025 (5) | 0.0075 (11) | 0.0036 (5) | -0.001 (1) | 0.0017 (9) | 0.000 (1) |
| B2 | 0.1550 (7) | 0.6540 (10) | 0.3324 (7) | 0.0056 (6) | 0.0065 (10) | 0.0032 (5) | 0.001 (1) | 0.0051 (8) | 0.000 (1) |
| B5 | 0.2618 (8) | 0.6303 (9) | 0.4342 (7) | 0.0060 (7) | 0.0058 (11) | 0.0027 (5) | -0.001 (2) | 0.0019 (10) | -0.002 (1) |
| B6 | 0.1906 (7) | 0.3800 (9) | 0.3511 (7) | 0.0050 (6) | 0.0051 (10) | 0.0035 (5) | -0.002 (1) | 0.0030 (9) | -0.000 (1) |
| B9 | 0.2903 (7) | 0.4689 (10) | 0.4430 (6) | 0.0044 (6) | 0.0069 (11) | 0.0025 (5) | 0.000 (1) | 0.0018 (9) | 0.002 (1) |
| B10 | 0.2881 (7) | 0.5924 (9) | 0.2202 (6) | 0.0048 (6) | 0.0055 (10) | 0.0037 (5) | 0.001 (1) | 0.0043 (8) | 0.002 (1) |
| B11 | 0.3782 (7) | 0.6022 (9) | 0.4181 (6) | 0.0040 (6) | 0.0049 (9) | 0.0035 (5) | 0.000 (1) | 0.0018 (9) | -0.001 (1) |
| B13 | 0.3659 (7) | 0.4500 (10) | 0.3083 (7) | 0.0046 (6) | 0.0060 (11) | 0.0035 (5) | -0.002 (1) | 0.0012 (9) | -0.002 (1) |
| H71 | 0.114 (7) | 0.170 (9) | 0.188 (6) | 5 | | | | | |
| H72 | 0.297 (7) | 0.103 (9) | 0.195 (6) | 5 | | | | | |
| H73 | 0.313 (6) | 0.362 (9) | 0.085 (6) | 5 | | | | | |
| H74 | 0.143 (6) | 0.468 (9) | 0.025 (6) | 5 | | | | | |
| H75 | 0.025 (7) | 0.365 (9) | 0.094 (6) | 5 | | | | | |
| H81 | 0.272 (7) | 0.907 (9) | 0.452 (6) | 5 | | | | | |
| H82 | 0.144 (7) | 0.926 (9) | 0.292 (6) | 5 | | | | | |
| H83 | 0.250 (7) | 0.900 (9) | 0.172 (6) | 5 | | | | | |
| H84 | 0.425 (7) | 0.887 (9) | 0.279 (6) | 5 | | | | | |
| H85 | 0.429 (7) | 0.879 (9) | 0.442 (6) | 5 | | | | | |
| H1 | 0.972 (5) | 0.002 (7) | 0.248 (5) | 4 (2) | | | | | |
| H2 | 0.914 (5) | 0.198 (7) | 0.166 (5) | 4 (2) | | | | | |
| H5 | 0.728 (5) | 0.333 (7) | 0.491 (5) | 4 (2) | | | | | |
| H6 | 0.153 (5) | 0.284 (7) | 0.370 (5) | 4 (2) | | | | | |
| H9 | 0.314 (6) | 0.421 (7) | 0.503 (5) | 6 (2) | | | | | |
| H10 | 0.701 (5) | 0.112 (7) | 0.360 (5) | 3 (2) | | | | | |
| H11 | 0.553 (5) | 0.387 (7) | 0.500 (5) | 6 (2) | | | | | |
| H13 | 0.880 (4) | 0.008 (6) | 0.052 (4) | 3 (2) | | | | | |

^a The form of the anisotropic thermal parameter is: $\exp[-(\beta_{11}h^2 + \beta_{22}k^2 + \beta_{33}l^2 + \beta_{12}hk + \beta_{13}hl + \beta_{23}kl)]$.

based on a bicapped hexagonal antiprism geometry. This forces the conclusion that, in the conversion from V to VII, *two nonadjacent carbons have in fact migrated to adjacent positions* in violation of the well-documented propensity of cage carbon atoms to move apart. The most likely explanation of this phenomenon is that the thermodynamic drive to achieve the symmetrical closo structure of VII predominates over the Coulombic repulsion between carbon nuclei, which in normal circumstances makes C-C bonds unfavorable in carborane frameworks.

The highly symmetrical structure of VIII (pseudo- D_{2d} point group), with its maximum separation of framework carbon atoms, suggested that VIII forms by rearrangement of VII. This was confirmed by subjecting a violet solution of VII in *n*-nonane to 300 °C for 3 h, which generated only the green isomer VIII accompanied by some decomposition. Thus we conclude that VIII is the final rearrangement product for this system.

Conclusions

The diagram in Figure 8 summarizes the observations de-

scribed above. Although the structure of the final isomer, VIII, is consistent with general trends previously observed in metallocarborane chemistry¹⁴—notably, the preference of metal atoms for high-coordinate vertices and the tendency of carbon atoms to migrate ultimately to nonvicinal locations—the stereochemistry of these 14-vertex polyhedra is novel in several respects. Perhaps most striking is the fact that, of the five structurally characterized isomers, no fewer than three kinds of polyhedra are represented. Thus, one class consists of the similar species I and V, a second type is exemplified by VII and VIII, and II forms yet another. This situation is unprecedented in carborane and metallocarborane chemistry, in that isomers normally adopt the same basic framework and differ only in the arrangement of heteroatoms on the polyhedral surface. The closest previously reported approach to a violation of this rule is given by the molecules¹⁵ *closo*- $[(CH_3)_3P]_2Pt(CH_3)_2C_2B_6H_6$ and *nido*- $[(C_2H_5)_3P]_2Pt(CH_3)_2C_2B_6H_6$, which are isomers save for the phosphino ligand groups, but have different gross geometries. However, the difference is not enormous, since the closo species is a tricapped trigonal prism and the nido system is a distorted tricapped trigonal prism in which one edge has

Table IV. Bond Distances (Å) for Cp₂Fe₂Me₄C₄B₈H₈ Isomers

| (a) Isomer I | | | | | | | |
|---------------|-----------|--------------|-----------|--------------|-----------|-------------|-----------|
| Fe(7)–C(4) | 2.138 (2) | Fe(8)–C(82) | 2.088 (2) | C(4)–CM(4) | 1.561 (2) | C(71)–C(72) | 1.418 (3) |
| Fe(7)–C(12) | 2.100 (2) | Fe(8)–C(83) | 2.122 (2) | C(4)–B(1) | 1.690 (3) | C(72)–C(73) | 1.413 (3) |
| Fe(7)–C(71) | 2.089 (2) | Fe(8)–C(84) | 2.116 (2) | C(4)–B(2) | 1.688 (3) | C(73)–C(74) | 1.384 (3) |
| Fe(7)–C(72) | 2.084 (2) | Fe(8)–C(85) | 2.081 (2) | C(4)–B(10) | 1.675 (3) | C(74)–C(75) | 1.397 (3) |
| Fe(7)–C(73) | 2.082 (2) | Fe(8)–B(2) | 2.110 (2) | C(11)–C(14) | 1.459 (2) | C(71)–C(75) | 1.401 (3) |
| Fe(7)–C(74) | 2.100 (2) | Fe(8)–B(5) | 2.144 (2) | C(11)–CM(11) | 1.532 (2) | C(81)–C(82) | 1.378 (3) |
| Fe(7)–C(75) | 2.100 (2) | Fe(8)–B(10) | 2.148 (2) | C(11)–B(5) | 1.616 (3) | C(82)–C(83) | 1.384 (3) |
| Fe(7)–B(1) | 2.098 (2) | C(83)–C(84) | 1.374 (3) | C(11)–B(9) | 1.959 (3) | B(2)–B(5) | 1.774 (3) |
| Fe(7)–B(6) | 2.124 (2) | C(84)–C(85) | 1.404 (3) | C(12)–CM(12) | 1.556 (2) | B(3)–B(6) | 1.773 (3) |
| Fe(7)–B(10) | 2.137 (2) | C(81)–C(85) | 1.424 (4) | C(12)–B(6) | 1.596 (2) | B(3)–B(9) | 1.797 (3) |
| Fe(7)–B(13) | 2.063 (2) | B(1)–B(2) | 1.775 (3) | C(12)–B(9) | 1.712 (3) | B(5)–B(9) | 1.852 (3) |
| Fe(8)–C(4) | 2.197 (2) | B(1)–B(3) | 1.756 (3) | C(12)–B(13) | 1.539 (3) | B(6)–B(9) | 1.880 (3) |
| Fe(8)–C(11) | 2.065 (2) | B(1)–B(6) | 1.764 (3) | C(14)–CM(14) | 1.545 (2) | B(10)–B(13) | 1.840 (3) |
| Fe(8)–C(14) | 2.015 (2) | B(2)–B(3) | 1.753 (3) | C(14)–B(10) | 1.656 (3) | Fe(7)–CP(7) | 1.720 |
| Fe(8)–C(81) | 2.065 (2) | | | C(14)–B(13) | 1.784 (2) | Fe(8)–CP(8) | 1.726 |
| (b) Isomer II | | | | | | | |
| Fe(7)–C(4) | 2.086 (4) | Fe(8)–C(83) | 2.077 (4) | Fe(8)–B(1) | 2.320 (4) | C(12)–B(5) | 1.685 (5) |
| Fe(7)–C(14) | 2.224 (3) | Fe(8)–C(84) | 2.081 (4) | Fe(8)–B(2) | 2.086 (4) | C(12)–B(6) | 1.703 (5) |
| Fe(7)–C(71) | 2.035 (5) | Fe(8)–C(85) | 2.097 (4) | Fe(8)–B(5) | 2.068 (4) | C(12)–B(9) | 1.757 (5) |
| Fe(7)–C(72) | 2.055 (5) | C(14)–CM(14) | 1.555 (4) | Fe(8)–B(10) | 2.186 (4) | B(1)–B(2) | 1.784 (5) |
| Fe(7)–C(73) | 2.068 (5) | C(14)–B(10) | 1.601 (5) | C(4)–CM(4) | 1.550 (5) | B(1)–B(3) | 1.897 (6) |
| Fe(7)–C(74) | 2.084 (6) | C(71)–C(72) | 1.348 (8) | C(4)–B(1) | 1.741 (5) | B(1)–B(10) | 1.998 (6) |
| Fe(7)–C(75) | 2.040 (5) | C(71)–C(75) | 1.337 (9) | C(4)–B(10) | 1.542 (5) | B(1)–B(13) | 2.095 (6) |
| Fe(7)–B(6) | 2.132 (4) | C(72)–C(73) | 1.34 (1) | C(4)–B(13) | 1.534 (6) | B(2)–B(3) | 1.743 (5) |
| Fe(7)–B(9) | 2.247 (4) | C(73)–C(74) | 1.31 (1) | C(11)–C(14) | 1.447 (4) | B(2)–B(5) | 1.764 (5) |
| Fe(7)–B(10) | 2.307 (4) | C(74)–C(75) | 1.28 (1) | C(11)–CM(11) | 1.564 (4) | B(3)–B(6) | 1.782 (6) |
| Fe(7)–B(13) | 2.187 (4) | C(81)–C(82) | 1.393 (7) | C(11)–B(5) | 1.642 (5) | B(3)–B(13) | 1.792 (6) |
| Fe(8)–C(11) | 2.090 (3) | C(81)–C(85) | 1.388 (6) | C(11)–B(9) | 1.735 (5) | B(5)–B(9) | 1.878 (5) |
| Fe(8)–C(14) | 2.083 (3) | C(82)–C(83) | 1.384 (7) | C(12)–CM(12) | 1.540 (5) | B(6)–B(9) | 1.760 (5) |
| Fe(8)–C(81) | 2.080 (4) | C(83)–C(84) | 1.406 (6) | C(12)–B(2) | 1.739 (5) | B(6)–B(13) | 1.745 (6) |
| Fe(8)–C(82) | 2.066 (4) | C(84)–C(85) | 1.387 (7) | C(12)–B(3) | 1.657 (5) | Fe(7)–CP(7) | 1.718 |
| | | | | | | Fe(8)–CP(8) | 1.710 |
| (c) Isomer V | | | | | | | |
| Fe(7)–C(4) | 2.155 (5) | C(4)–B(10) | 1.651 (6) | Fe(8)–CP(6) | 2.027 (5) | C(81)–C(82) | 1.32 (9) |
| Fe(7)–C(12) | 2.092 (4) | C(12)–CM(12) | 1.567 (5) | Fe(8)–CP(7) | 2.062 (5) | C(81)–C(85) | 1.25 (8) |
| Fe(7)–CP(1) | 2.074 (6) | C(12)–B(6) | 1.562 (6) | Fe(8)–CP(8) | 2.078 (5) | C(82)–C(83) | 1.37 (9) |
| Fe(7)–CP(2) | 2.089 (6) | C(12)–B(9) | 1.700 (6) | Fe(8)–CP(9) | 2.037 (5) | C(83)–C(84) | 1.33 (8) |
| Fe(7)–CP(3) | 2.116 (6) | C(12)–B(13) | 1.556 (6) | Fe(8)–CP(10) | 2.004 (5) | C(84)–C(85) | 1.27 (9) |
| Fe(7)–CP(4) | 2.074 (6) | C(14)–CM(14) | 1.577 (5) | Fe(8)–B(2) | 2.057 (5) | B(1)–B(2) | 1.790 (6) |
| Fe(7)–CP(5) | 2.052 (6) | C(14)–B(10) | 1.583 (6) | Fe(8)–B(5) | 2.115 (5) | B(1)–B(6) | 1.807 (6) |
| Fe(7)–B(1) | 2.062 (5) | C(14)–B(11) | 1.558 (6) | Fe(8)–B(10) | 2.171 (5) | B(2)–B(5) | 1.755 (6) |
| Fe(7)–B(6) | 2.100 (5) | C(14)–B(13) | 1.676 (6) | Fe(8)–B(11) | 2.168 (5) | B(5)–B(9) | 1.745 (7) |
| Fe(7)–B(10) | 2.213 (5) | C(71)–C(72) | 1.41 (1) | C(3)–CM(3) | 1.592 (6) | B(5)–B(11) | 1.757 (7) |
| Fe(7)–B(13) | 2.222 (5) | C(72)–C(73) | 1.39 (1) | C(4)–CM(4) | 1.569 (6) | B(6)–B(9) | 1.851 (7) |
| Fe(8)–C(4) | 2.193 (4) | C(73)–C(74) | 1.40 (1) | C(4)–B(1) | 1.681 (6) | B(9)–B(11) | 1.985 (7) |
| Fe(8)–C(14) | 2.027 (4) | C(74)–C(75) | 1.40 (1) | C(4)–B(2) | 1.729 (6) | B(10)–B(13) | 2.048 (8) |
| | | C(75)–C(71) | 1.40 (1) | | | Fe(7)–CP(7) | 1.707 |
| | | | | | | Fe(8)–CP(8) | 1.712 |

been stretched to a nonbonding (2.48 Å) B–B distance.¹⁵ This type of distortion is not uncommon in platinacarboranes¹⁶ and has been attributed¹⁷ to unequal bonding capabilities of the 5d_{xz} and 5d_{yz} orbitals on platinum.

In the (η^5 -C₅H₅)₂Fe₂(CH₃)₄C₄B₈H₈ systems, which are precisely isomeric, the considerable variation in polyhedral shape is not likely to be explained in electronic terms; all other known metallocarboranes of first-row transition elements are well-behaved, in the sense that the skeletal electron-counting rules^{8,9} are strictly obeyed. Hence we believe that we are dealing with kinetic effects related to the extreme size of the polyhedra and the mode of insertion of the metal ions into the (CH₃)₄C₄B₈H₈²⁻ dianion. That is to say, although the symmetrical closo geometry of Figure 1 is preferred thermodynamically, the kinetics of metal insertion are such that the polyhedron is locked into an open position. It will be noted that the nido species I, II, and V each contain two framework atoms, one boron and one carbon, which are bound to both metals; VII and VIII have no such feature. In order to achieve the geometry

of VII, therefore, at least two Fe–B/C links in V must be broken, a fairly drastic operation which evidently entails high activation energy and does not occur at an appreciable rate below 300 °C.

A number of unanswered questions remain, a principal one being the extent to which these phenomena might be general for 14-vertex systems, as opposed to M₂C₄B₈ species specifically. The persistence of the nido geometry below 300 °C suggests that steric effects of this type are likely to be encountered in other 14-vertex (or larger) systems, and may in fact be characteristic of such cages.

Finally, we note that from the viewpoint of the skeletal electron-counting theory, isomers I, II, and V (and probably III and IV also) constitute a new class of polyhedra: cages for which closo geometry is favored (2n + 2 skeletal electrons), but which are effectively frozen into nido configurations for steric reasons. Such cases might conveniently be designated pseudo-nido to distinguish them from true nido species (2n + 4 electrons). It is possible that the pseudo-nido geometry of

Table V. Bond Angles (deg) for Cp₂Fe₂Me₄C₄B₈H₈ Isomers

| | | (a) Isomer I | |
|--------------------|------------|--------------------|------------|
| C(4)-Fe(7)-C(12) | 102.30 (7) | Fe(7)-B(6)-B(3) | 113.4 (1) |
| C(4)-Fe(7)-B(1) | 47.02 (8) | Fe(7)-B(6)-B(9) | 106.4 (1) |
| C(4)-Fe(7)-B(6) | 87.21 (8) | C(12)-B(6)-B(1) | 119.0 (2) |
| C(4)-Fe(7)-B(10) | 46.12 (7) | C(12)-B(6)-B(3) | 113.4 (2) |
| C(4)-Fe(7)-B(13) | 90.25 (7) | C(12)-B(6)-B(9) | 58.4 (1) |
| C(12)-Fe(7)-B(1) | 87.24 (8) | B(1)-B(6)-B(3) | 59.5 (1) |
| C(12)-Fe(7)-B(6) | 44.39 (7) | C(14)-Fe(8)-B(2) | 107.49 (7) |
| C(12)-Fe(7)-B(10) | 86.48 (7) | C(14)-Fe(8)-B(5) | 81.99 (7) |
| C(12)-Fe(7)-B(13) | 43.37 (7) | C(14)-Fe(8)-B(10) | 46.74 (7) |
| B(1)-Fe(7)-B(6) | 49.38 (8) | B(2)-Fe(8)-B(5) | 49.28 (8) |
| B(1)-Fe(7)-B(10) | 88.28 (8) | B(2)-Fe(8)-B(10) | 86.27 (8) |
| B(1)-Fe(7)-B(13) | 109.11 (8) | B(5)-Fe(8)-B(10) | 98.50 (8) |
| B(6)-Fe(7)-B(10) | 105.52 (8) | Fe(7)-C(4)-Fe(8) | 123.15 (8) |
| B(6)-Fe(7)-B(13) | 84.05 (8) | Fe(7)-C(4)-CM(4) | 113.8 (1) |
| B(10)-Fe(7)-B(13) | 51.93 (8) | Fe(7)-C(4)-B(1) | 65.23 (9) |
| C(4)-Fe(8)-C(11) | 99.03 (7) | Fe(7)-C(4)-B(2) | 119.2 (1) |
| C(4)-Fe(8)-C(14) | 85.92 (6) | Fe(7)-C(4)-B(10) | 66.90 (9) |
| C(4)-Fe(8)-B(2) | 46.10 (8) | Fe(8)-C(4)-CM(4) | 113.1 (1) |
| C(4)-Fe(8)-B(5) | 83.48 (7) | Fe(8)-C(4)-B(1) | 120.3 (1) |
| C(4)-Fe(8)-B(10) | 45.32 (7) | Fe(8)-C(4)-B(2) | 64.22 (9) |
| C(11)-Fe(8)-C(14) | 41.88 (7) | Fe(8)-C(4)-B(10) | 65.78 (9) |
| C(11)-Fe(8)-B(2) | 88.62 (8) | CM(4)-C(4)-B(1) | 113.1 (1) |
| C(11)-Fe(8)-B(5) | 45.11 (7) | CM(4)-C(4)-B(2) | 114.6 (1) |
| C(11)-Fe(8)-B(10) | 80.10 (7) | CM(4)-C(4)-B(10) | 114.2 (1) |
| Fe(8)-C(11)-B(9) | 113.9 (1) | B(1)-C(4)-B(2) | 63.4 (1) |
| C(14)-C(11)-CM(11) | 118.5 (2) | B(1)-C(4)-B(10) | 122.4 (1) |
| C(14)-C(11)-B(5) | 125.2 (2) | B(2)-C(4)-B(10) | 119.9 (1) |
| C(14)-C(11)-B(9) | 108.1 (1) | Fe(8)-C(11)-C(14) | 67.24 (9) |
| CM(11)-C(11)-B(5) | 114.2 (2) | Fe(8)-C(11)-CM(11) | 126.8 (1) |
| CM(11)-C(11)-B(9) | 113.1 (1) | Fe(8)-C(11)-B(5) | 70.0 (1) |
| B(5)-C(11)-B(9) | 61.5 (1) | C(72)-C(71)-C(75) | 107.7 (2) |
| Fe(7)-C(12)-CM(12) | 124.1 (1) | C(71)-C(72)-C(73) | 106.4 (2) |
| Fe(7)-C(12)-B(6) | 68.6 (1) | C(72)-C(73)-C(74) | 109.5 (2) |
| Fe(7)-C(12)-B(9) | 114.2 (1) | C(73)-C(74)-C(75) | 107.6 (2) |
| Fe(7)-C(12)-B(13) | 67.0 (1) | C(71)-C(75)-C(74) | 108.9 (2) |
| CM(12)-C(12)-B(6) | 112.0 (2) | C(82)-C(81)-C(85) | 107.1 (2) |
| CM(12)-C(12)-B(9) | 117.4 (2) | C(81)-C(82)-C(83) | 109.0 (2) |
| CM(12)-C(12)-B(13) | 116.5 (2) | C(82)-C(83)-C(84) | 108.8 (2) |
| B(6)-C(12)-B(9) | 69.2 (1) | C(83)-C(84)-C(85) | 108.0 (2) |
| B(6)-C(12)-B(13) | 104.8 (1) | C(81)-C(85)-C(84) | 107.1 (2) |
| Fe(8)-C(14)-C(11) | 70.88 (9) | Fe(7)-B(1)-C(4) | 67.75 (9) |
| Fe(8)-C(14)-CM(14) | 122.0 (1) | Fe(7)-B(1)-B(2) | 117.1 (1) |
| Fe(8)-C(14)-B(10) | 70.84 (9) | Fe(7)-B(1)-B(3) | 115.4 (1) |
| Fe(8)-C(14)-B(13) | 124.3 (1) | Fe(7)-B(1)-B(6) | 66.09 (9) |
| C(11)-C(14)-CM(14) | 119.5 (2) | C(4)-B(1)-B(2) | 58.3 (1) |
| C(11)-C(14)-B(10) | 120.9 (1) | C(4)-B(1)-B(3) | 107.2 (1) |
| C(11)-C(14)-B(13) | 105.5 (1) | C(4)-B(1)-B(6) | 116.6 (1) |
| CM(14)-C(14)-B(10) | 118.7 (2) | B(2)-B(1)-B(3) | 59.6 (1) |
| CM(14)-C(14)-B(13) | 108.2 (1) | B(2)-B(1)-B(6) | 111.9 (2) |
| B(10)-C(14)-B(13) | 64.6 (1) | B(3)-B(1)-B(6) | 60.5 (1) |
| B(1)-B(3)-B(2) | 60.8 (1) | Fe(8)-B(2)-C(4) | 69.68 (9) |
| B(1)-B(3)-B(5) | 111.3 (2) | Fe(8)-B(2)-B(1) | 120.8 (1) |
| B(1)-B(3)-B(6) | 60.0 (1) | Fe(8)-B(2)-B(3) | 118.7 (1) |
| B(1)-B(3)-B(9) | 107.6 (1) | Fe(8)-B(2)-B(5) | 66.37 (9) |
| B(2)-B(3)-B(5) | 60.9 (1) | C(4)-B(2)-B(1) | 58.4 (1) |
| B(2)-B(3)-B(6) | 112.5 (2) | C(4)-B(2)-B(3) | 107.4 (1) |
| B(2)-B(3)-B(9) | 109.1 (1) | C(4)-B(2)-B(5) | 113.2 (1) |
| B(5)-B(3)-B(6) | 118.0 (1) | B(1)-B(2)-B(3) | 59.7 (1) |
| B(5)-B(3)-B(9) | 63.0 (1) | B(1)-B(2)-B(5) | 109.2 (2) |
| B(6)-B(3)-B(9) | 63.5 (1) | B(3)-B(2)-B(5) | 59.4 (1) |
| Fe(8)-B(5)-C(11) | 64.85 (9) | B(1)-B(6)-B(9) | 103.7 (1) |
| Fe(8)-B(5)-B(2) | 64.4 (1) | B(3)-B(6)-B(9) | 58.9 (1) |
| Fe(8)-B(5)-B(3) | 117.3 (1) | C(11)-B(9)-C(12) | 103.1 (1) |
| Fe(8)-B(5)-B(9) | 115.0 (1) | C(11)-B(9)-B(3) | 103.6 (1) |
| C(11)-B(5)-B(2) | 118.6 (2) | C(11)-B(9)-B(5) | 50.09 (9) |
| C(11)-B(5)-B(3) | 122.8 (2) | C(11)-B(9)-B(6) | 128.9 (1) |
| C(11)-B(5)-B(9) | 68.4 (1) | C(12)-B(9)-B(3) | 106.8 (1) |
| B(2)-B(5)-B(3) | 59.7 (1) | C(12)-B(9)-B(5) | 130.8 (2) |
| B(2)-B(5)-B(9) | 105.8 (1) | C(12)-B(9)-B(6) | 52.5 (1) |
| B(3)-B(5)-B(9) | 59.8 (1) | B(3)-B(9)-B(5) | 57.2 (1) |
| Fe(7)-B(6)-C(12) | 67.01 (9) | B(3)-B(9)-B(6) | 57.6 (1) |
| Fe(7)-B(6)-B(1) | 64.5 (1) | B(5)-B(9)-B(6) | 107.9 (1) |

Table V (continued)

| | | | |
|--------------------|------------|--------------------|-----------|
| Fe(7)–B(10)–Fe(8) | 125.72 (9) | C(14)–B(10)–B(13) | 61.1 (1) |
| Fe(7)–B(10)–C(4) | 67.98 (9) | Fe(7)–B(13)–C(12) | 69.6 (1) |
| Fe(7)–B(10)–C(14) | 117.2 (1) | Fe(7)–B(13)–C(14) | 114.9 (1) |
| Fe(7)–B(10)–B(13) | 61.97 (9) | Fe(7)–B(13)–B(10) | 66.10 (9) |
| Fe(8)–B(10)–C(4) | 68.90 (9) | C(12)–B(13)–C(14) | 116.9 (2) |
| Fe(8)–B(10)–C(14) | 62.42 (9) | C(12)–B(13)–B(10) | 118.1 (2) |
| Fe(8)–B(10)–B(13) | 114.6 (1) | C(14)–B(13)–B(10) | 54.4 (1) |
| C(4)–B(10)–C(14) | 119.3 (1) | CP (7)–CP (8) | 57.4 |
| C(4)–B(10)–B(13) | 115.8 (1) | | |
| (b. Isomer II) | | | |
| C(4)–Fe(7)–C(14) | 81.4 (1) | B(1)–B(3)–B(2) | 58.5 (2) |
| C(4)–Fe(7)–B(6) | 84.8 (2) | B(1)–B(3)–B(6) | 104.9 (3) |
| C(4)–Fe(7)–B(9) | 108.9 (1) | B(1)–B(3)–B(13) | 69.1 (3) |
| C(4)–Fe(7)–B(10) | 40.7 (1) | B(2)–B(3)–B(6) | 107.5 (3) |
| C(4)–Fe(7)–B(13) | 42.0 (2) | B(2)–B(3)–B(13) | 119.7 (3) |
| C(14)–Fe(7)–B(6) | 105.5 (1) | B(6)–B(3)–B(13) | 58.4 (2) |
| C(14)–Fe(7)–B(9) | 70.0 (1) | Fe(8)–B(5)–C(11) | 67.5 (2) |
| C(14)–Fe(7)–B(10) | 41.3 (1) | Fe(8)–B(5)–C(12) | 116.9 (2) |
| C(14)–Fe(7)–B(13) | 108.9 (1) | Fe(8)–B(5)–B(2) | 65.4 (2) |
| B(6)–Fe(7)–B(10) | 102.2 (1) | Fe(8)–B(5)–B(9) | 109.1 (2) |
| B(6)–Fe(7)–B(13) | 47.6 (2) | C(11)–B(5)–C(12) | 114.1 (3) |
| B(9)–Fe(7)–B(10) | 94.5 (1) | C(11)–B(5)–B(2) | 118.7 (3) |
| B(9)–Fe(7)–B(13) | 89.0 (2) | C(11)–B(5)–B(9) | 58.8 (2) |
| B(10)–Fe(7)–B(13) | 76.8 (2) | C(12)–B(5)–B(2) | 60.5 (2) |
| C(11)–Fe(8)–C(14) | 40.6 (1) | C(12)–B(5)–B(9) | 59.0 (2) |
| C(11)–Fe(8)–B(1) | 101.0 (1) | B(2)–B(5)–B(9) | 104.1 (2) |
| C(11)–Fe(8)–B(2) | 89.1 (1) | Fe(7)–B(6)–C(12) | 118.0 (2) |
| C(11)–Fe(8)–B(5) | 46.5 (1) | Fe(7)–B(6)–B(3) | 113.3 (2) |
| C(11)–Fe(8)–B(10) | 123.9 (2) | Fe(7)–B(6)–B(9) | 69.8 (2) |
| C(14)–Fe(8)–B(1) | 87.5 (1) | Fe(7)–B(6)–B(13) | 67.8 (2) |
| C(14)–Fe(8)–B(2) | 107.7 (1) | C(12)–B(6)–B(3) | 56.7 (2) |
| C(14)–Fe(8)–B(5) | 83.2 (1) | C(12)–B(6)–B(9) | 61.0 (2) |
| C(14)–Fe(8)–B(10) | 44.0 (1) | C(12)–B(6)–B(13) | 113.1 (3) |
| B(1)–Fe(8)–B(2) | 47.4 (2) | C(4)–B(13)–B(3) | 111.6 (3) |
| B(1)–Fe(8)–B(5) | 87.7 (1) | C(4)–B(13)–B(6) | 120.1 (3) |
| B(1)–Fe(8)–B(10) | 52.5 (1) | B(1)–B(13)–B(3) | 57.8 (2) |
| CM(12)–C(12)–B(6) | 118.1 (3) | B(2)–Fe(8)–B(5) | 50.3 (2) |
| CM(12)–C(12)–B(9) | 118.8 (3) | B(2)–Fe(8)–B(10) | 94.2 (2) |
| B(2)–C(12)–B(3) | 61.7 (2) | B(5)–Fe(8)–B(10) | 106.1 (2) |
| B(2)–C(12)–B(5) | 62.0 (2) | Fe(7)–C(4)–CM(4) | 131.2 (3) |
| B(2)–C(12)–B(6) | 111.4 (3) | Fe(7)–C(4)–B(1) | 109.2 (2) |
| B(2)–C(12)–B(9) | 110.1 (2) | Fe(7)–C(4)–B(10) | 77.4 (2) |
| B(3)–C(12)–B(5) | 118.6 (3) | Fe(7)–C(4)–B(13) | 72.5 (2) |
| B(3)–C(12)–B(6) | 64.1 (2) | CM(4)–C(4)–B(1) | 119.6 (3) |
| B(3)–C(12)–B(1) | 114.6 (3) | CM(4)–C(4)–B(10) | 113.8 (3) |
| B(5)–C(12)–B(6) | 118.9 (3) | CM(4)–C(4)–B(13) | 115.7 (3) |
| B(5)–C(12)–B(9) | 65.8 (2) | B(1)–C(4)–B(10) | 74.7 (3) |
| B(6)–C(12)–B(9) | 61.1 (2) | B(1)–C(4)–B(13) | 79.3 (3) |
| Fe(7)–C(14)–Fe(8) | 116.6 (1) | B(10)–C(4)–B(13) | 130.5 (3) |
| Fe(7)–C(14)–C(11) | 95.4 (2) | Fe(8)–C(11)–C(14) | 69.5 (2) |
| Fe(7)–C(14)–CM(14) | 119.7 (2) | Fe(8)–C(11)–CM(11) | 126.8 (2) |
| Fe(7)–C(14)–B(10) | 72.1 (2) | Fe(8)–C(11)–B(5) | 66.1 (2) |
| Fe(8)–C(14)–C(11) | 70.0 (2) | Fe(8)–C(11)–B(9) | 113.8 (2) |
| Fe(8)–C(14)–CM(14) | 121.9 (2) | C(14)–C(11)–CM(11) | 117.7 (3) |
| Fe(8)–C(14)–B(10) | 71.4 (2) | C(14)–C(11)–B(5) | 126.2 (3) |
| C(11)–C(14)–CM(14) | 116.4 (3) | C(14)–C(11)–B(9) | 107.0 (3) |
| C(11)–C(14)–B(10) | 127.7 (3) | CM(11)–C(11)–B(5) | 112.7 (3) |
| CM(14)–C(14)–B(10) | 113.6 (3) | CM(11)–C(11)–B(9) | 113.1 (3) |
| C(72)–C(71)–C(75) | 107.3 (6) | B(5)–C(11)–B(9) | 67.2 (2) |
| C(71)–C(72)–C(73) | 106.1 (6) | CM(12)–C(12)–B(12) | 122.1 (3) |
| C(72)–C(73)–C(74) | 109.2 (7) | CM(12)–C(12)–B(3) | 116.8 (3) |
| C(73)–C(74)–C(75) | 107.0 (6) | CM(12)–C(12)–B(5) | 112.6 (3) |
| C(71)–C(75)–C(74) | 108.2 (6) | Fe(8)–B(1)–C(4) | 106.8 (2) |
| C(85)–C(81)–C(82) | 108.2 (5) | Fe(8)–B(1)–B(2) | 59.4 (2) |
| C(81)–C(82)–C(83) | 108.5 (4) | Fe(8)–B(1)–B(3) | 109.0 (2) |
| C(82)–C(83)–C(84) | 107.2 (4) | Fe(8)–B(1)–B(10) | 60.3 (2) |
| C(83)–C(84)–C(85) | 108.3 (4) | Fe(8)–B(1)–B(13) | 124.8 (2) |
| C(81)–C(85)–C(84) | 107.8 (4) | C(4)–B(1)–B(2) | 135.4 (3) |
| B(3)–B(2)–B(5) | 110.0 (3) | C(4)–B(1)–B(3) | 98.3 (3) |
| C(12)–B(3)–B(1) | 106.6 (3) | C(4)–B(1)–B(10) | 48.1 (2) |
| C(12)–B(3)–B(2) | 61.5 (2) | C(4)–B(1)–B(13) | 46.0 (2) |
| C(12)–B(3)–B(6) | 59.2 (2) | B(2)–B(1)–B(3) | 56.4 (2) |
| C(12)–B(3)–B(13) | 113.0 (3) | B(2)–B(1)–B(10) | 111.6 (3) |

Table V (continued)

| | | | |
|--------------------|-----------|-------------------|-----------|
| B(2)-B(1)-B(13) | 103.7 (3) | C(11)-B(9)-B(6) | 131.7 (3) |
| B(3)-B(1)-B(10) | 123.3 (3) | C(12)-B(9)-B(5) | 55.2 (2) |
| B(3)-B(1)-B(13) | 53.1 (2) | C(12)-B(9)-B(6) | 57.9 (2) |
| B(10)-B(1)-B(13) | 86.0 (2) | B(5)-B(9)-B(6) | 106.9 (3) |
| Fe(8)-B(2)-C(12) | 113.5 (2) | Fe(7)-B(10)-Fe(8) | 109.3 (2) |
| Fe(8)-B(2)-B(1) | 73.2 (2) | Fe(7)-B(10)-C(4) | 61.9 (2) |
| Fe(8)-B(2)-B(3) | 127.8 (2) | Fe(7)-B(10)-C(14) | 66.5 (2) |
| Fe(8)-B(2)-B(5) | 64.4 (2) | Fe(7)-B(10)-B(1) | 92.9 (2) |
| C(12)-B(2)-B(1) | 108.2 (3) | Fe(8)-B(10)-C(4) | 122.2 (3) |
| C(12)-B(2)-B(3) | 56.8 (2) | Fe(8)-B(10)-C(14) | 64.6 (2) |
| C(12)-B(2)-B(5) | 57.5 (2) | Fe(8)-B(10)-B(1) | 67.2 (2) |
| B(1)-B(2)-B(3) | 65.1 (2) | C(4)-B(10)-C(14) | 126.7 (3) |
| B(1)-B(2)-B(5) | 118.2 (3) | C(4)-B(10)-B(1) | 57.2 (2) |
| B(3)-B(6)-B(9) | 108.4 (3) | C(14)-B(10)-B(1) | 115.3 (3) |
| B(3)-B(6)-B(13) | 61.1 (2) | Fe(7)-B(13)-C(4) | 65.5 (2) |
| B(9)-B(6)-B(13) | 124.9 (3) | Fe(7)-B(13)-B(1) | 93.8 (2) |
| Fe(7)-B(9)-C(11) | 87.0 (2) | Fe(7)-B(13)-B(3) | 110.4 (2) |
| Fe(7)-B(9)-C(12) | 110.1 (2) | Fe(7)-B(13)-B(6) | 64.5 (2) |
| Fe(7)-B(9)-B(5) | 118.8 (2) | C(4)-B(13)-B(1) | 54.7 (2) |
| Fe(7)-B(9)-B(6) | 62.9 (2) | B(3)-B(13)-B(6) | 60.5 (2) |
| C(11)-B(9)-C(12) | 106.1 (3) | B(1)-B(13)-B(6) | 98.5 (3) |
| C(11)-B(9)-B(5) | 54.0 (2) | CP(7)-CP(8) | 41.1 |
| (c) Isomer V | | | |
| C(4)-Fe(7)-C(12) | 102.4 (4) | C(3)-B(5)-B(9) | 60.0 (3) |
| C(4)-Fe(7)-B(1) | 46.9 (3) | C(3)-B(5)-B(11) | 120.8 (3) |
| C(4)-Fe(7)-B(6) | 88.9 (4) | B(2)-B(5)-B(9) | 108.3 (3) |
| C(12)-Fe(7)-B(1) | 88.0 (4) | B(2)-B(5)-B(11) | 119.0 (4) |
| C(12)-Fe(7)-B(6) | 43.7 (3) | B(9)-B(5)-B(11) | 69.1 (3) |
| B(1)-Fe(7)-B(6) | 51.5 (3) | Fe(7)-B(6)-C(3) | 110.4 (3) |
| C(4)-Fe(8)-C(14) | 83.3 (3) | Fe(7)-B(6)-C(12) | 67.9 (3) |
| C(4)-Fe(8)-B(2) | 47.9 (3) | Fe(7)-B(6)-B(1) | 63.2 (3) |
| C(4)-Fe(8)-B(5) | 84.6 (3) | Fe(7)-B(6)-B(9) | 108.1 (3) |
| C(4)-Fe(8)-B(10) | 44.5 (2) | C(3)-B(6)-C(12) | 111.2 (4) |
| C(4)-Fe(8)-B(11) | 98.3 (3) | C(3)-B(6)-B(1) | 58.1 (3) |
| C(14)-Fe(8)-B(2) | 110.3 (3) | C(3)-B(6)-B(9) | 57.5 (3) |
| C(14)-Fe(8)-B(5) | 86.8 (3) | C(12)-B(6)-B(1) | 117.8 (3) |
| C(14)-Fe(8)-B(10) | 44.1 (3) | C(12)-B(6)-B(9) | 59.0 (3) |
| C(14)-Fe(8)-B(11) | 43.4 (3) | B(1)-B(6)-B(9) | 103.4 (3) |
| B(2)-Fe(8)-B(5) | 49.8 (2) | C(3)-B(9)-C(12) | 104.7 (4) |
| B(2)-Fe(8)-B(10) | 88.2 (2) | C(3)-B(9)-B(5) | 58.7 (3) |
| B(2)-Fe(8)-B(11) | 91.5 (3) | C(3)-B(9)-B(6) | 57.5 (3) |
| B(5)-Fe(8)-B(10) | 101.0 (3) | CM(3)-C(3)-B(2) | 115.7 (4) |
| B(5)-Fe(8)-B(11) | 48.4 (3) | CM(3)-C(3)-B(5) | 117.4 (4) |
| B(10)-Fe(8)-B(11) | 79.1 (3) | CM(3)-C(3)-B(6) | 114.3 (4) |
| CM(3)-C(3)-B(1) | 117.3 (4) | CM(3)-C(3)-B(9) | 120.9 (4) |
| CM(4)-C(4)-B(1) | 110.2 (4) | B(1)-C(3)-B(2) | 63.6 (3) |
| CM(4)-C(4)-B(2) | 112.2 (4) | B(1)-C(3)-B(5) | 114.8 (3) |
| CM(4)-C(4)-B(10) | 114.2 (4) | B(1)-C(3)-B(6) | 63.4 (3) |
| B(1)-C(4)-B(2) | 63.3 (3) | B(1)-C(3)-B(9) | 113.3 (3) |
| B(1)-C(4)-B(10) | 126.2 (3) | B(2)-C(3)-B(5) | 62.5 (3) |
| B(2)-C(4)-B(10) | 121.2 (3) | B(2)-C(3)-B(6) | 118.8 (3) |
| Fe(7)-C(12)-CM(12) | 124.1 (4) | B(2)-C(3)-B(9) | 112.8 (3) |
| Fe(7)-C(12)-B(6) | 68.4 (3) | B(5)-C(3)-B(6) | 118.6 (3) |
| Fe(7)-C(12)-B(9) | 114.9 (3) | B(5)-C(3)-B(9) | 61.3 (3) |
| Fe(7)-C(12)-B(13) | 73.4 (3) | B(6)-C(3)-B(9) | 65.0 (3) |
| CM(12)-C(12)-B(6) | 112.8 (4) | Fe(7)-C(4)-Fe(8) | 122.1 (2) |
| CM(12)-C(12)-B(9) | 116.8 (4) | Fe(7)-C(4)-CM(4) | 117.4 (4) |
| CM(12)-C(12)-B(13) | 113.3 (4) | Fe(7)-C(4)-B(1) | 63.6 (3) |
| B(6)-C(12)-B(9) | 69.0 (3) | Fe(7)-C(4)-B(2) | 116.2 (3) |
| B(6)-C(12)-B(13) | 131.2 (3) | Fe(7)-C(4)-B(10) | 69.7 (3) |
| B(9)-C(12)-B(13) | 102.7 (3) | Fe(8)-C(4)-B(1) | 118.6 (3) |
| Fe(8)-C(14)-CM(14) | 122.1 (4) | Fe(8)-C(4)-B(2) | 61.9 (3) |
| Fe(8)-C(14)-B(10) | 72.8 (3) | Fe(8)-C(4)-B(10) | 67.1 (3) |
| Fe(8)-C(14)-B(11) | 73.1 (3) | C(72)-C(71)-C(75) | 106.9 (8) |
| Fe(8)-C(14)-B(13) | 126.2 (3) | C(71)-C(72)-C(73) | 109.7 (8) |
| CM(14)-C(14)-B(10) | 117.4 (4) | C(72)-C(73)-C(74) | 106.4 (8) |
| CM(14)-C(14)-B(11) | 119.0 (4) | C(73)-C(74)-C(75) | 109.5 (8) |
| CM(14)-C(14)-B(13) | 111.3 (4) | C(71)-C(75)-C(74) | 107.4 (7) |
| B(10)-C(14)-B(11) | 123.3 (3) | C(82)-C(81)-C(85) | 109.9 (6) |
| B(10)-C(14)-B(13) | 77.8 (3) | C(81)-C(82)-C(83) | 106.6 (6) |
| B(11)-C(14)-B(13) | 87.7 (3) | C(82)-C(83)-C(84) | 103.6 (6) |
| Fe(8)-B(5)-C(3) | 115.0 (4) | C(83)-C(84)-C(85) | 110.6 (6) |
| Fe(8)-B(5)-B(2) | 63.4 (3) | | |
| Fe(8)-B(5)-B(9) | 120.3 (3) | | |
| Fe(8)-B(5)-B(11) | 67.4 (3) | | |
| C(3)-B(5)-B(2) | 58.2 (3) | | |

Table V (continued)

| | | | |
|-------------------|-----------|-------------------|-----------|
| C(81)-C(85)-C(84) | 109.2 (5) | C(12)-B(9)-B(5) | 128.6 (3) |
| Fe(7)-B(1)-C(3) | 112.5 (3) | C(12)-B(9)-B(6) | 52.0 (3) |
| Fe(7)-B(1)-C(4) | 69.4 (4) | C(12)-B(9)-B(11) | 94.2 (3) |
| Fe(7)-B(1)-B(2) | 118.0 (3) | B(5)-B(9)-B(6) | 109.8 (3) |
| Fe(7)-B(1)-B(6) | 65.4 (3) | B(5)-B(9)-B(11) | 55.8 (3) |
| C(3)-B(1)-C(4) | 106.3 (3) | B(6)-B(9)-B(11) | 126.5 (3) |
| C(3)-B(1)-B(2) | 57.3 (3) | Fe(8)-B(10)-C(4) | 68.5 (3) |
| C(3)-B(1)-B(6) | 58.5 (3) | Fe(8)-B(10)-C(14) | 63.1 (3) |
| C(4)-B(1)-B(2) | 59.6 (3) | Fe(8)-B(10)-B(13) | 103.1 (3) |
| C(4)-B(1)-B(6) | 117.3 (3) | C(4)-B(10)-C(14) | 120.4 (3) |
| B(2)-B(1)-B(6) | 109.1 (3) | C(4)-B(10)-B(13) | 111.4 (3) |
| Fe(8)-B(2)-C(3) | 118.8 (4) | C(14)-B(10)-B(13) | 53.1 (3) |
| Fe(8)-B(2)-C(4) | 70.2 (3) | Fe(8)-B(11)-C(14) | 63.5 (3) |
| Fe(8)-B(2)-B(1) | 120.4 (3) | Fe(8)-B(11)-B(5) | 64.2 (3) |
| Fe(8)-B(2)-B(5) | 66.8 (3) | Fe(8)-B(11)-B(9) | 107.6 (3) |
| C(3)-B(2)-C(4) | 105.5 (3) | C(14)-B(11)-B(5) | 118.3 (4) |
| C(3)-B(2)-B(1) | 59.1 (3) | C(14)-B(11)-B(9) | 116.1 (4) |
| C(3)-B(2)-B(5) | 59.3 (3) | B(5)-B(11)-B(9) | 55.2 (3) |
| C(4)-B(2)-B(1) | 57.0 (3) | C(12)-B(13)-C(14) | 127.9 (3) |
| C(4)-B(2)-B(5) | 112.6 (4) | C(12)-B(13)-B(10) | 114.8 (3) |
| B(1)-B(2)-B(5) | 108.5 (3) | C(14)-B(13)-B(10) | 49.1 (3) |
| C(3)-B(9)-B(11) | 108.2 (3) | CP(7)-CP(8) | 50.6 |

these systems can be exploited as a route to even larger cages, examples of which are presently unknown. Both I and V have well-defined five-membered open faces, into which a two-electron donor metal group such as $(\eta^5\text{-C}_5\text{H}_5)\text{Co}$ might be inserted to generate a 15-vertex $\text{CoFe}_2\text{C}_4\text{B}_8$ polyhedron having a true $(2n + 2)$ -electron closo structure.

Synthetic studies along this line are currently in progress.

Experimental Section

Materials. The metallocarborane isomers I and II were obtained as described elsewhere.^{1a} Thin layer and preparative-layer chromatography of product mixtures were conducted on precoated plates of silica gel F-254 purchased from Brinckmann Instruments, Inc. Solvents were reagent grade and used as received.

Spectra. Boron-11 NMR spectra at 32.1 MHz and proton NMR spectra at 100 MHz were obtained on a Jeol PS-100P pulse Fourier transform instrument.

Rearrangement of $(\eta^5\text{-C}_5\text{H}_5)_2\text{Fe}_2(\text{CH}_3)_4\text{C}_4\text{B}_8\text{H}_8$ (isomer I) to isomer V. A 5-mg sample of I was dissolved in 0.5-mL of *n*-nonane and heated in vacuo in a Pyrex tube for 6 h at 164 °C. TLC analysis of the mixture using hexane revealed the presence of one new isomer (V) in addition to the starting material. The solution was then heated at 170 °C for an additional 7.5 h, after which TLC analysis in hexane showed that only V was present. No other isomers and essentially no decomposition were detected. The product, V, was obtained by distilling off the nonane under vacuum, dissolving in methylene chloride, and chromatographing on a preparative-layer silica gel plate in hexane to give 5 mg of brown crystals. The mass spectrum of V was nearly identical with those of I and II.^{1a} The boron-11 NMR spectrum of V in CDCl_3 exhibited doublets at δ 24.1 ppm relative to $\text{BF}_3\cdot\text{O}(\text{C}_2\text{H}_5)_2$ ($J_{\text{BH}} = 137$ Hz), 19.9 (185), 13.4 (157), 9.2 (127), 5.5 (136), 2.7 (115), and -12.4 (156), with relative areas of 1:1:1:1:2:1:1. *Positive sign indicates shift to lower field.*¹⁸ The 100-MHz proton NMR spectrum of V in CDCl_3 contains C_5H_5 resonances at δ 4.57 and 4.43 ppm relative to Me_4Si (positive sign indicates shift to lower field), and CH_3 resonances at δ 2.82, 1.98, 1.85, and 1.49. In toluene- d_8 the C_5H_5 peaks appear at δ 4.25 and 4.14, and the CH_3 resonances are at δ 2.91, 2.23, 1.67, and 1.57.

Rearrangement of II to V. A solution of II (2 mg) in toluene- d_8 was placed in a thick-walled 5-mm diameter NMR tube in vacuo and heated at 140 °C for 4 h. At this point the NMR spectrum was recorded, revealing that none of the original species^{1a} remained. Two new isomers, V and VI, were evident in a ratio of ~1:4. Further heating at 140 °C for 4 h resulted in a V:VI ratio of 1:2. After an additional 12-h period at 150 °C, the NMR spectrum indicated that the mixture was 95% V. The tube was opened, solvent was removed, and the solid residue was chromatographed on a TLC plate in hexane to yield 2 mg of dark brown crystals of V. From the NMR spectra, color, and R_f value it was evident that V was identical with the product obtained by thermal isomerization of I as described above.

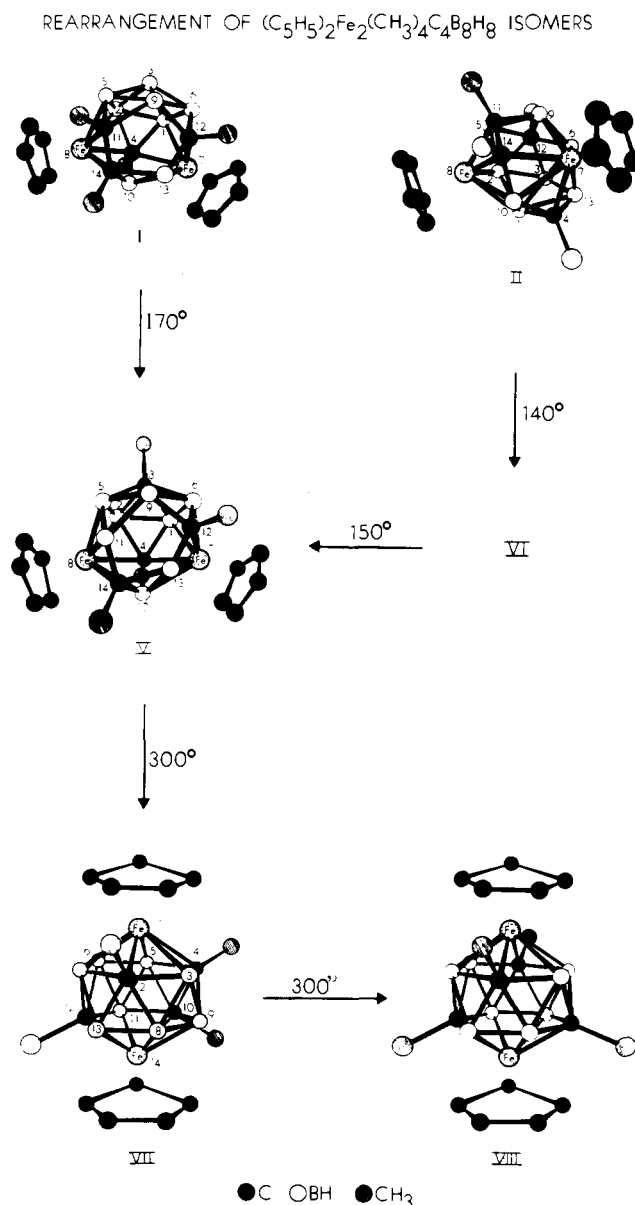


Figure 8. Thermal rearrangement of $(\eta^5\text{-C}_5\text{H}_5)_2\text{Fe}_2(\text{CH}_3)_4\text{C}_4\text{B}_8\text{H}_8$ isomers. Structures of I, II, V, and VIII are established, and that of VII is proposed from NMR data.

The intermediate VI was not isolated, but its spectrum contained C_5H_5 resonances at δ 4.27 and 3.99 and CH_3 peaks at δ 2.51 (2 CH_3), 1.46, and 1.41.

Rearrangement of V to VII. A solution of 5 mg of isomer V in degassed *n*-nonane was sealed into an evacuated thick-walled 5-mm Pyrex NMR tube and heated at 200 °C for 90 min with no change in the ^{11}B NMR spectrum (described above). An additional 2 h at 220 °C also produced no change in the spectrum, but further heating at 250 °C for 60 min caused a small shoulder to appear at δ -18 ppm;¹⁸ otherwise, the spectrum was identical with that of V. A final heating period at 300 °C for 60 min produced a complete transformation of the spectrum, and at this point the tube was opened and separated on a TLC plate in 35% benzene in hexane. Three main bands were obtained, consisting of unreacted V (~20%), violet VII (~60%), and green VIII (~20%); a minute trace of an unidentified yellow material was also observed. The ^{11}B NMR spectrum of VII in $CDCl_3$ contained heavily overlapped doublets at δ -12.8 ppm ($J = 145$ Hz), -17.5 (146), and -19.7 (186), with relative areas 1:2:1 (again, negative sign denotes shift to higher field¹⁸); the assignment of chemical shifts was facilitated by proton decoupling, which produced singlet resonances with the indicated chemical shifts. The area 2 peak arises from superposition of two signals, as shown by the fact that four different BH peaks are observed in the ^{11}B -decoupled proton spectrum. The 1H spectrum in $CDCl_3$ exhibited a single C_5H_5 resonance at δ 4.15, methyl peaks of equal area at δ 2.08 and 1.84, and ^{11}B decoupling revealed B-H peaks of equal area at δ 3.07, 2.52, 2.38, and 1.92.

The ^{11}B NMR spectrum of VIII consisted of one doublet at δ -18.0 ppm ($J = 152$ Hz), while the 1H spectrum exhibited a C_5H_5 peak at δ 4.29 and a methyl resonance at 2.17 ppm. The proton-decoupled ^{11}B spectrum consisted of a singlet at δ -18.0 with a half-width of only 2.1 ppm, unusually sharp for a metallocarborane ^{11}B resonance.

Rearrangement of VII to VIII. A solution of VII in degassed *n*-nonane was sealed into an evacuated thick-walled NMR tube and heated at 300 °C for 3 h, during which the original violet solution turned green. TLC separation of the mixture indicated that partial decomposition had occurred to give nonmobile degradation products. The remaining isomer mixture consisted of about 75% VIII and 25% VII, identified from their TLC behavior and NMR spectra. No evidence of any other isomers was found.

X-Ray Crystallographic Studies of ($\eta^5-C_5H_5$) $_2Fe_2(CH_3)_4C_4B_8H_8$ Isomers I, II, and V. Crystal data for isomer I: mol wt 445, space group $P2_1/n$, $Z = 4$, $a = 10.676(2)$, $b = 14.009(5)$, $c = 13.669$ Å, $\beta = 93.97(3)^\circ$, $V = 2039$ Å³, $d_{\text{calcd}} = 1.45$ g cm⁻³ (densities were not measured for any of the isomers due to paucity of material and the fact that the molecular formulas were well established from NMR and mass spectra); $\mu(\text{Mo K}\alpha) = 14.6$ cm⁻¹; crystal dimensions (distances in millimeters of faces from centroid): (001) 0.095, (00 $\bar{1}$) 0.095, (010) 0.25, (0 $\bar{1}$ 0) 0.25, (10 $\bar{1}$) 0.20, ($\bar{2}$ 11) 0.20. $P2_1/n$ is an alternative setting of the conventional space group $P2_1/c$ and has the general equivalent position $x, y, z, \bar{x}, \bar{y}, \bar{z}; \frac{1}{2} + x, \frac{1}{2} - y, \frac{1}{2} + z; \frac{1}{2} + y, \frac{1}{2} - z$. The transformation matrix for conversion of the present setting into the conventional one is

$$\begin{pmatrix} 1 & 0 & 0 \\ 0 & 1 & 0 \\ -1 & 0 & 1 \end{pmatrix}$$

Thus the cell parameters in $P2_1/c$ (a_c, b_c, c_c, β_c) derived from those given for $P2_1/n$ (a_n, b_n, c_n, β_n) have $a_c = a_n, b_c = b_n$, while $c_c = 17.917(7)$ Å and $\beta_c = 130.44(3)^\circ$.

Crystal data for isomer II: mol wt 445, space group $C2/c$, $Z = 8$, $a = 16.338(3)$, $b = 8.210(2)$, $c = 31.55(1)$ Å, $\beta = 103.74(2)^\circ$, $V = 4111$ Å³, $d_{\text{calcd}} = 1.44$ g cm⁻³, $\mu(\text{Mo K}\alpha) = 14.5$ cm⁻¹; crystal dimensions (millimeters from centroid): (101) 0.115, ($\bar{1}$ 0 $\bar{1}$) 0.115, (10 $\bar{1}$) 0.11, ($\bar{1}$ 01) 0.11, ($\bar{1}$ 10) 0.125, ($\bar{1}$ 10) 0.125, (001) 0.05, (00 $\bar{1}$) 0.05.

Crystal data for isomer V: mol wt 445, space group $P2_1/c$, $Z = 4$, $a = 14.805(4)$, $b = 10.547(2)$, $c = 14.682(5)$ Å, $\beta = 109.20(2)^\circ$, $V = 2060$ Å³, $d_{\text{calcd}} = 1.44$ g cm⁻³, $\mu(\text{Mo K}\alpha) = 14.5$ cm⁻¹, crystal dimensions (millimeters from centroid): (100) 0.005, ($\bar{1}$ 00) 0.005, (010) 0.19, (0 $\bar{1}$ 0) 0.19, (011) 0.10, (0 $\bar{1}$ 1) 0.10.

For each crystal, the Enraf-Nonius program SEARCH was used to obtain 15 accurately centered reflections which were then used in the program INDEX to obtain an orientation matrix for data collection and also approximate cell dimensions. Refined cell dimensions and their estimated standard deviations were obtained from least-squares

refinement of 28 accurately centered reflections. The mosaicity of each crystal was examined by the ω -scan technique and judged to be satisfactory.

Collection and Reduction of Data. Diffraction data were collected at 292 K on an Enraf-Nonius four-circle CAD-4 diffractometer controlled by a PDP8/M computer, using Mo $K\alpha$ radiation from a highly oriented graphite crystal monochromator. The θ - 2θ scan technique was used to record the intensities for all nonequivalent reflections for which $1^\circ < 2\theta < 47^\circ$, $1^\circ < 2\theta < 48^\circ$, and $1^\circ < 2\theta < 44^\circ$ for isomers I, II, and V respectively. Scan widths (SW) were calculated from the formula $SW = A + B \tan \theta$, where A is estimated from the mosaicity of the crystal and B allows for the increase in width of peak due to $K\alpha_1$ - $K\alpha_2$ splitting. The values of A and B were 0.70 and 0.30°, respectively, for isomer I, and 0.60 and 0.30 for isomers II and V. The calculated scan angle was extended at each side by 25% for background determination (BG1 and BG2). The net count was then calculated at $NC = \text{TOT} - 2(\text{BG1} + \text{BG2})$ where TOT is the integrated peak intensity. Reflection data were considered insignificant if intensities registered less than ten counts above background on a rapid prescan, such reflections being rejected automatically by the computer.

The intensities of four standard reflections, monitored for each crystal at 100-reflection intervals, showed no greater fluctuations during the data collection than those expected from Poisson statistics. The raw intensity data were corrected for Lorentz-polarization effects and then for absorption. After averaging the intensities of equivalent reflections, the data were reduced to 3069 independent intensities for isomer I, 3149 for isomer II, and 2651 for isomer V, of which 2796 for isomer I, 2403 for isomer II, and 1661 for isomer V had $F_o^2 > 3\sigma(F_o^2)$, where $\sigma(F_o^2)$ was estimated from counting statistics.¹⁹ These data were used in the final refinement of the structural parameters.

Determination and Refinement of the Structures. The positions of the iron atoms were determined in each of the compounds from three-dimensional Patterson functions calculated from all intensity data. For each crystal the intensity data were phased sufficiently well by these positional coordinates to permit location of the remaining nonhydrogen and some hydrogen atoms.

Full-matrix least-squares refinement was based on F , and the function minimized was $\sum w(|F_o| - |F_c|)^2$. The weights w were then taken as $[2F_o/\sigma(F_o^2)]^2$, where $|F_o|$ and $|F_c|$ are the observed and calculated structure factor amplitudes. The atomic scattering factors for nonhydrogen atoms were taken from Cromer and Waber,²⁰ and those for hydrogen from Stewart et al.²¹ The effects of anomalous dispersion for all nonhydrogen atoms were included in F_c using the values of Cromer and Ibers²² for $\Delta f'$ and $\Delta f''$. Agreement factors are defined as $R = \sum |F_o| - |F_c| / \sum |F_o|$ and $R_w = (\sum w(|F_o| - |F_c|)^2 / \sum w|F_o|^2)^{1/2}$. To minimize computer time, the initial calculations were carried out on the first 1000 reflections collected.

Anisotropic temperature factors were introduced for all nonhydrogen atoms, and the cyclopentadienyl hydrogen atoms were included as fixed atoms at the calculated positions, with isotropic temperature factors of 5.0 Å², assuming C-H = 0.95 Å. Further Fourier difference maps permitted location of the remaining nonmethyl hydrogen atoms, which were included as isotropic atoms for three cycles of refinement and thereafter held fixed. The models converged with $R = 4.1$, $R_w = 6.2\%$; $R = 4.2$, $R_w = 5.9\%$; and $R = 4.7$, $R_w = 5.7\%$ for isomers I, II, and V, respectively. A structure factor calculation with all observed and unobserved reflections included (no refinement) gave $R = 4.9\%$ for isomer I, $R = 5.0\%$ for isomer II, and $R = 5.3\%$ for isomer V. On this basis it was decided that careful measurement of reflections rejected automatically during data collections would not significantly improve the results. Final Fourier difference maps were featureless. Tables of the observed structure factors are available.²³

The molecules are well-separated in all three structures, the nearest intermolecular contacts being those between methyl or cyclopentadienyl groups. The closest nonhydrogen atom approaches are as follows: in isomer I, C(75) and C(84) of adjacent molecules are 3.558(3) Å apart; in II, C(71) and C(75) (symmetry operation $\frac{1}{2} - x, \frac{1}{2} - y, \frac{1}{2} - z$) are separated by 3.424(8) Å; and in V, two C3M atoms (symmetry operation $-x, 1 - y, 1 - z$) are 3.23(1) Å apart.

Acknowledgment. This work was supported in part by the Office of Naval Research and in part by the National Science Foundation, Grant No. CHE 76-04491. The Fourier transform NMR spectrometer and associated computer were obtained

in part through a departmental grant from the National Science Foundation.

Supplementary Material Available: Listings of observed and calculated structure factors (34 pages). Ordering information is given on any current masthead page.

References and Notes

- (1) (a) Part 1: W. M. Maxwell, R. F. Bryan, and R. N. Grimes, *J. Am. Chem. Soc.*, preceding paper in this issue; (b) presented in part at the Third International Meeting on Boron Chemistry, Munich, Germany, July 1976.
- (2) (a) W. M. Maxwell, V. R. Miller, and R. N. Grimes, *J. Am. Chem. Soc.*, **96**, 7116 (1974); (b) W. M. Maxwell, V. R. Miller, and R. N. Grimes, *Inorg. Chem.*, **15**, 1343 (1976).
- (3) (a) R. Weiss, D. Freyberg, E. Sinn, and R. N. Grimes, *Inorg. Chem.*, in press; (b) R. Weiss and R. N. Grimes, to be submitted for publication.
- (4) W. J. Evans and M. F. Hawthorne, *J. Chem. Soc., Chem. Commun.*, 38 (1974).
- (5) Throughout this article we designate the isomers of $(\eta^5\text{-C}_5\text{H}_5)_2\text{Fe}_2\text{-(CH}_3)_4\text{C}_4\text{B}_8\text{H}_8$ by Roman numerals, rather than following the usual practice⁶ of distinguishing isomers by heteroatom locations [as in 1,8,5,6-(C₅H₅)₂Co₂C₂B₅H₇]. In the 14-vertex cages discussed here, the variation in gross geometry and the irregular nature of the polyhedra make it essentially meaningless to designate and compare isomers by heteroatom numbering. This will be true of any set of isomers lacking a common polyhedral framework.
- (6) International Union of Pure and Applied Chemistry, *Pure Appl. Chem.*, **30**, 683 (1972).
- (7) W. M. Maxwell, E. Sinn, and R. N. Grimes, *J. Chem. Soc., Chem. Commun.*, 389 (1976).
- (8) K. Wade, *Adv. Inorg. Chem. Radiochem.*, **18**, 1 (1976).
- (9) R. W. Rudolph and W. R. Pretzer, *Inorg. Chem.*, **11**, 1974 (1972).
- (10) W. N. Lipscomb, "Boron Hydrides", W. A. Benjamin, New York, N.Y., 1963, p 92.
- (11) For a comprehensive review of metallocarborane chemistry, see R. N. Grimes in "Organometallic Reactions and Syntheses", Vol. 6, Plenum Publishing Co., New York, N.Y., 1977, Chapter 2, pp 63-221.
- (12) R. E. Williams, *Adv. Inorg. Chem. Radiochem.*, **18**, 67 (1976).
- (13) J. R. Pipal and R. N. Grimes, to be submitted for publication.
- (14) (a) M. K. Kaloustian, R. J. Wiersema, and M. F. Hawthorne, *J. Am. Chem. Soc.*, **94**, 6679 (1972); (b) D. F. Dustin, W. J. Evans, C. J. Jones, R. J. Wiersema, H. Gong, S. Chan, and M. F. Hawthorne, *ibid.*, **96**, 3085 (1974); (c) W. J. Evans, C. J. Jones, B. Stlbr, and M. F. Hawthorne, *J. Organomet. Chem.*, **60**, C27 (1973); (d) V. R. Miller and R. N. Grimes, *J. Am. Chem. Soc.*, **97**, 4213 (1975).
- (15) M. Green, J. L. Spencer, F. G. A. Stone, and A. J. Welch, *J. Chem. Soc., Chem. Commun.*, 794 (1974).
- (16) (a) M. Green, J. L. Spencer, F. G. A. Stone, and A. J. Welch, *J. Chem. Soc., Dalton Trans.*, 179 (1975); (b) A. J. Welch, *ibid.*, 1473 (1975); (c) W. E. Carroll, M. Green, F. G. A. Stone, and A. J. Welch, *ibid.*, 2263 (1975); (d) A. J. Welch, *ibid.*, 2270 (1975); (e) M. Green, J. A. K. Howard, J. L. Spencer, and F. G. A. Stone, *ibid.*, 2274 (1975); (f) A. J. Welch, *ibid.*, 225 (1976).
- (17) D. M. P. Mingos, *J. Chem. Soc., Dalton Trans.*, 602 (1977).
- (18) The new ¹¹B NMR sign convention employed here is discussed in ref 1a, footnote 17.
- (19) P. W. R. Corfield, R. J. Doedens, and J. A. Ibers, *Inorg. Chem.*, **6**, 197 (1967).
- (20) D. T. Cromer and J. T. Waber, "International Tables for X-Ray Crystallography", Vol. IV, Kynoch Press, Birmingham, England, 1974.
- (21) R. F. Stewart, E. R. Davidson, and W. T. Simpson, *J. Chem. Phys.*, **42**, 3175 (1965).
- (22) D. T. Cromer and J. A. Ibers, "International Tables for X-Ray Crystallography", Vol. IV, Kynoch Press, Birmingham, England, 1974.
- (23) Supplementary material.

Ring Size Effects among Metal Complexes with Macrocyclic Ligands: Synthesis, Stereochemistry, Spectrochemistry, and Electrochemistry of Cobalt(III) Complexes with Unsubstituted, Saturated Tetraaza Macrocycles

Yann Hung, Ludmila Y. Martin, Susan C. Jackels, A. Martin Tait, and Daryle H. Busch*

Contribution from the Evans Chemical Laboratory, The Ohio State University, Columbus, Ohio 43210. Received October 10, 1976

Abstract: A series of fully saturated, unsubstituted, tetraaza macrocyclic ligands, varying in ring size from 13 to 16 members, has been used to evaluate the relationships between ring size and such properties as ligand field strengths and redox potentials of complexes. Cobalt(III) complexes of the general formula $\text{Co}([13\text{-}16]\text{aneN}_4)\text{X}_n^+$ have been synthesized, where $[13]\text{aneN}_4$, $[14]\text{aneN}_4$, $[15]\text{aneN}_4$, and $[16]\text{aneN}_4$ are the saturated macrocyclic ligands and X_n are Cl_2 , Br_2 , $(\text{N}_3)_2$, $(\text{NCS})_2$, $(\text{CN})_2$, or CO_3 . Both cis and trans isomers could be prepared with $[13]\text{aneN}_4$, but only the trans geometry was found for the complexes of $[15]\text{aneN}_4$ and $[16]\text{aneN}_4$, except for the cis complexes with bidentate CO_3^{2-} . $[14]\text{aneN}_4$ has been studied earlier. The secondary amine groups are chiral and exhibit configurational integrity when coordinated to Co^{3+} . This results in the existence of configurational isomers of both *trans*- $\text{Co}([15]\text{aneN}_4)\text{Cl}_2^+$ and *trans*- $\text{Co}([16]\text{aneN}_4)\text{Cl}_2^+$, which have been separated and characterized. Strain energy calculations, ¹³C NMR spectra, and chemical properties are used to deduce the detailed structures of these configurational isomers. The spectrochemical consequences of ring size are revealed in the variations of the ligand field parameters Dq^{xy} (due to macrocyclic ligand field) and Dq^z (due to monodentate axial ligands). Dq^{xy} varies with the macrocycles in the order $13 > 14 > 15 > 16$. The ligand $[14]\text{aneN}_4$ exhibits a Dq^{xy} value that is normal for saturated amines—that ring size fits Co^{3+} best. The smaller ring $[13]\text{aneN}_4$ exerts a constrictive effect on the metal ion because of excess strain energy. This produces an enhancement in Dq^{xy} . The large rings, $[15]\text{aneN}_4$ and $[16]\text{aneN}_4$, are caused by strain energy effects to exert a dilative effect on the $\text{Co}^{3+}\text{-N}$ linkages, thereby producing a diminished ligand field (Dq^{xy}). Dq^{xy} also differs among configurational isomers. The range of Dq^{xy} spanned with the ligands $[13\text{-}16]\text{aneN}_4$ is 511 cm^{-1} for the trans isomers, while Dq^{xy} only ranges over 144 cm^{-1} for the cis isomers (carbonates). The redox potentials for the *trans*- $\text{Cl}_2\text{Co}^{3+}$ complexes follow the trend in strain energy rather than the trend in Dq^{xy} . Thus Co^{3+} is most stable in *trans*- $\text{Co}([14]\text{aneN}_4)\text{Cl}_2^+$ and least stable in *trans*- $\text{Co}([16]\text{aneN}_4)\text{Cl}_2^+$. The geometric constraints that relate to the fit between a metal ion and a given size of macrocyclic ligand provide some of the most distinctive relationships among these substances.

The occurrence of macrocyclic ligands in the structures of a number of the most prominent biologically important, natural complexes strongly implies that there are significant

advantages in the macrocyclic ligand structure. The importance of ring size is equally apparent in the occurrence of a 16-membered inner ring in the porphyrin ligand of the heme